Hamline University
DigitalCommons@Hamline

Departmental Honors Projects | College of Liberal Arts

Spring 2015

The Significance of CRISPR/Cas9-Directed CUL3 Knockout on Human Colorectal Cancer Cells

Zoe A. Lautz
Hamline University

Follow this and additional works at: https://digitalcommons.hamline.edu/dhp

Part of the Biotechnology Commons, Cancer Biology Commons, Cell Biology Commons, Digestive System Diseases Commons, Education Commons, Genetics Commons, Laboratory and Basic Science Research Commons, Molecular Biology Commons, and the Other Cell and Developmental Biology Commons

Recommended Citation
Lautz, Zoe A., "The Significance of CRISPR/Cas9-Directed CUL3 Knockout on Human Colorectal Cancer Cells" (2015). *Departmental Honors Projects*. 40.
https://digitalcommons.hamline.edu/dhp/40

This Honors Project is brought to you for free and open access by the College of Liberal Arts at DigitalCommons@Hamline. It has been accepted for inclusion in Departmental Honors Projects by an authorized administrator of DigitalCommons@Hamline. For more information, please contact digitalcommons@hamline.edu, lterveer01@hamline.edu.

The Significance of CRISPR/Cas9-Directed CUL3 Knockout on Human Colorectal Cancer Cells

Zoe Lautz

An Honors Thesis Submitted
for partial fulfillment of the requirements for graduation with honors in
Biology from Hamline University

April 23, 2014

TABLE OF CONTENTS

ABSTRACT

Cancer, the second leading cause of death in the US, is caused by mutations in select genes that alter cellular function leading to uncontrolled proliferation. Understanding the specific genes that drive cancer can lead to the generation of novel cancer therapies. To identify novel genes that drive cancer in the colon (CRC), lungs, and ovaries in mice, Starr et al. employed a transposon-based insertional mutagenesis system. One of the genes identified, APC, is mutated in 70-80% of human CRCs. CUL3, suspected to be a general driver gene, was discovered in the lung cancer screen. CUL3 was analyzed for its role in a human CRC cell line in this study. CUL3 gene knockout was performed using the CRISPR/Cas9 system, which targets mutations to specific genes, thereby knocking out that gene's function. Three different sites in the CUL3 gene were targeted for mutation and resulted in the creation of 41 separate cell lines with potential CUL3 knockout. Of those 41 cell lines, 25 exhibited qualitatively abnormal phenotypes 10 days after transfection. These phenotypes include slowed growth (25 of 25 cell lines), increased cell size (16 of 25 cell lines), and variation of cell adherence to culture flask surface (11 of 25 cell lines). Knockout was confirmed in 6 cell lines by using PCR in the region of the gene targeted for mutation and sequencing the PCR product. Each cell line was quantitatively evaluated for metabolic activity (or cell growth rate) using an MTS assay. If CUL3 knockout is shown to reduce overall cell growth and increase susceptibility to chemotherapy, this would support the development of new therapies for CRCs that target CUL3 function.

INTRODUCTION

PROJECT SIGNIFICANCE

Cancer is as pervasive as it is destructive. As the second leading cause of death in the US, it has become a ubiquitous danger in today's society (Murphy et al. 2013). Colorectal cancer (cancer of either the colon or rectum) is the third most common cancer in both sexes, after breast/prostate and lung cancers. According to the American Cancer Society, in 2014 an estimated 96,830 new cases of colon cancer will be diagnosed, and 50,310 people are expected to die of this disease. In an individual's lifetime, it is estimated that they will have a 1 in 20 chance of developing colorectal cancer. That's 5% of the US population (American Cancer Society).

Current colon cancer treatments include surgery, radiation therapies, and chemotherapy. Surgery is used to remove the portion of bowel that contains the tumor and is most the effective treatment at earlier stage cancers. Radiation therapies use high energy light rays to destroy the cancer cells. This is most commonly used when the tumor is in later stages and has invaded another internal organ or abdomen lining, where surgery would be more difficult. It is also commonly used when the cancer has spread, especially when it has spread to the bones or brain, sites that are inoperable. Chemotherapy is the administration of drugs designed to kill quickly dividing cells. In colorectal cancer, chemotherapy is mainly administered to patients post-surgery to rid the body of any remaining tumor cells, as well as to those in advanced stages to lengthen life-expectancy (American Cancer Society). These particular chemotherapies include standard rapid growth inhibitors, like capecitabine (the first line treatment) and irinotecan (a second line treatment), which inhibit RNA synthesis and DNA replication, respectively. They also include monoclonal antibodies, which target epidermal growth factor receptors (EGFRs), often

overexpressed in colorectal cancer, but which are only effective in cancers overexpressing EGFRs (Cortejoso & Lopez-Fernandez 2012).

Depending on the stage, certain treatments are more effective. Stage I is almost exclusively treated with surgery, and has a 5 year survival rate of 74%. Stages II and III usually is a combination of treatments, with surgery when possible and radiation when not, as well as chemotherapy. Both of these stages range in survival rates (II: 37%-67%; III: 28%-73%) depending on the location of the tumor, the amount the tumor has invaded into other organs, and whether or not it has reached the lymph system. Stage IV is the most fatal, as the cancer has already spread to other organs and is often inoperable, which is why chemotherapy is often given to slow the growth of the cancer. The survival rate for this cancer is 6% (American Cancer Society).

Cancer is the result of multiple mutations (about 5-10) in select genes that allow cells to rapidly divide and consume the body's resources. These "driver" genes have often been reduced to oncogenes and tumor suppressors, where oncogenes gain function to induce tumorigenesis and tumor suppressors lose function to allow growth (Vogelstein & Kinzler 2004). However, with the boom of genetic study following the Human Genome Project, other classes of genes that affect tumorigenic growth have been identified. Hanahan and Weinberg have published more than one paper entitled *Hallmarks of Cancer* with the goal of classifying potential tumorigenic genes or cellular properties and widening our understanding of the genetic causes to cancer. In their latest edition, published in 2011, they add four more hallmarks, bringing the total to 10. These include, but are not limited to, properties that induce angiogenesis, increase genome instability, resist growth suppressors, and avoid immune response. By recognizing the driver

genes that allow tumorigenic growth, we can specifically target the effects of these genes to create swifter and more effective treatment.

The most famous (and very effective) targeted cancer driver therapy is the drug Herceptin. It specifically interferes with the gene HER2, which is commonly mutated in breast cancer, as well as other cancers. The mutation results in the overexpression of the HER2 protein receptor on the outside of the cells that, when activated, signals the cell to start dividing. Herceptin interrupts this pathway by blocking the receptor so that the cell cannot receive the signal to divide. The drug has been shown to be extremely effective on late-stage and spreading cancers, helping those who would not benefit from more traditional therapies. (Herceptin).

This research, like the Herceptin research, could be the stepping stone to creating more specific cancer drugs with fewer side effects. By knowing what genetic mutations help or hinder tumorigenesis, we may be able target those pathways to slow the cancer's growth, giving patients more time and options.

TRANSPOSON-BASED INSERTIONAL MUTAGENESIS

Transposon-Based Insertional Mutagenesis

There are various ways to induce tumorigenesis in models to study cancer. Until recently retroviral insertional mutagenesis was the method of choice, as it allowed for rapid tumor induction and high throughput. However, this method is not truly random, as the proviral DNA has tendencies to integrate at the 5' ends of genes. It can also affect the promotion of oncogenes hundreds of kilobases away by way of an enhancer within the proviral DNA, making it difficult to determine which gene the insertion is truly affecting (Copeland and Jenkins 2010). Since this method of tumorigenesis does not lend itself to accurate biostatistical analysis, another rapid,

high-throughput method was needed. It was found in transposon-based insertional mutagenesis (TIM).

DNA-only transposons are short segments of DNA that can move randomly within the genome. Traditionally, these transposons move on their own, coding for their own excision and integration enzyme, called a transposase, within the transposable element. However, non-autonomous transposons have been experimentally created, and are able to be controlled by providing the transposase in *trans*, i.e. separate from the transposable element (Copeland and Jenkins 2010). Multiple copies of the transposon within the genome ensures high rates of mutative transposition, as there is a 30-40% chance that the transposon will not reintegrate after excision (Copeland and Jenkins 2010).

The Sleeping Beauty (SB) transposon is one of those that have been used to induce cancer in mice. It was originally seen in fish, *xenopus*, and even human genomes, however, generations of mutations left the transposase catalytically inactive. Ivics et al. (1997) reconstructed the transposase and "awoke" the transposon from evolutionary sleep, allowing its transposition to occur again. Its mobility in mammalian species made it an excellent candidate for alteration for research use.

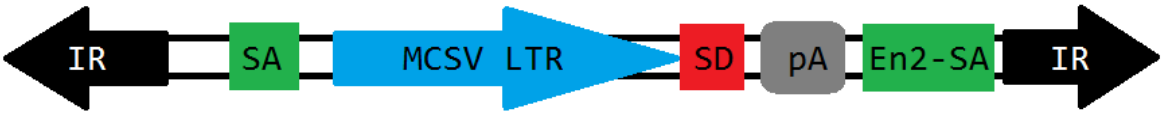

Figure 1. *The layout of the T2/Onc2 transposon.* The DNA-only transposon is capped with inverted repeats (the black arrows at the ends) and includes two splicing acceptor sites (SA) and a splicing donor site (SD); a murine stem cell virus (MCSV LTR) promoter; and a poly-adenine tail sequence (pA).

To utilize the SB transposon as a cancer inducer, Dupuy et al. created the T2/Onc2 transposon (2005) (Figure 1). It contains a murine stem cell virus long terminal repeat (MSCV LTR) to activate transcription and a polyadenylation tail to signal the early termination of

transcription. Splice donor and splice acceptor sites are to alter the splicing of the mRNA product of the intended targets. Breeding the T2/Onc2 transgenic mice with another transgenic strain, known as RosaSB, which expressed the SB11 transposase ubiquitously in all tissues, led to double transgenic mice that have the ability to mobilize the T2/Onc2 transposon. Unfortunately (or fortunately) for Dupuy et al., the transposon/transposase combination worked too well – many transgenic mice died as embryos due to lethal mutations caused by the transposon system (2005). Of the 24 mice that survived weaning, all had died of cancer (mostly blood cancers) by 17 weeks.

Transposon Use for Discovery of CRC Driver Genes

In 2009, Dr. Starr and a team of researchers at the University of Minnesota published a paper that utilized TIM to create a murine model of colorectal cancer. They bred a line of transgenic mice from three others: RosaSB, VillinCre, and T2/Onc. The RosaSB and VillinCre mice were first bred together. The offspring from this mating had transposase expression that was exclusive to the epithelium of the colon. This double-transgenic mouse was then bred with the T2/Onc mouse to create the triple-transgenic line that contained the directed transposase and 25 copies of the T2/Onc2 transposon. The mice were then watched for 18 months, or until they passed away from colorectal cancer at which time the tumors were then harvested and genotyped. The location of each transposon insertion was determined. Genomic analysis was performed on all insertion sites and a catalogue of driver versus passenger mutation was created based off of biostatistics on the likelihood of multiple insertions being randomly close together in the genome. Of the 135 tumors harvested, 16,690 insertion sites were catalogued. From thse insertion sites, 77 genes were found to be likely colorectal cancer driver genes.

One gene of note discovered in this system was the APC gene. This gene is found in over 70% of colorectal cancers and serves as a proof-of-concept discovery. While many of the genes identified have already been catalogued, many had not been previously linked to colorectal cancer.

Dr. Starr has since repeated this process in lung and ovarian cancers in mice (Starr, unpublished). CUL3 was found to be a driver gene in lung cancers, though further study indicates that CUL3 may be a general cancer driver gene, and was hence used in this study to determine if it may have a role in CRC development.

CUL3 FUNCTION AND ITS POTENTIAL ROLE IN CANCER

Ubiquitination and Protein Degradation

Ubiquitination is the process of attaching the small protein, called ubiquitin, to a protein to affect its function. The attachment of ubiquitin to target proteins involves three mediating enzymes: ubiquitin-activating enzyme (E1), ubiquitin-conjugating enzyme (E2), and ubiquitin ligase (E3) (Figure 2). While there are few types of E1 and E2s, E3s are the most diverse group of ubiquitination enzymes, with over 500 E3 ligases identified (Andérica-Romero et al. 2013). The more common process of polyubiquitination marks proteins for degradation, while monoubiquitination is

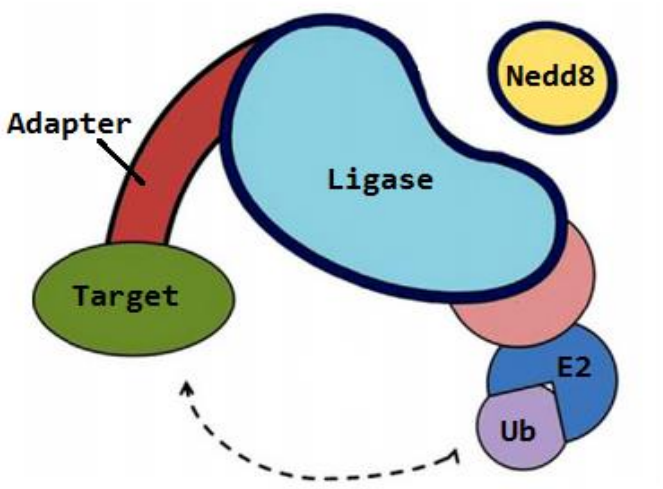

Figure 2. *Schematic of Ubiquitin Ligation*. (Adapted from Andérica-Romero et al. 2013) Ubiquitination requires more than just the ligase. Above, the ligase uses an adapter to bind to the target protein. Nedd8 is a neddylation factor (see pg. 12) that alters ligase function, Ub is the ubiquitin, and E2 is the Ub-conjugating enzyme.

occasionally used to alter the function of or localize certain proteins (less is known about monoubiquitination).

Ubiquitin-dependent degradation is performed by the 26S proteasome complex. The complex is a conglomeration of proteases that create a cylindrical tube of catalytic activity, capped by a regulatory "lid" that protects cytosolic proteins from accidentally entering the catalytic cylinder. The proteasome lid recognizes the ubiquitin and unwinds the target protein, feeding it through the cylinder, where the protein is degraded into short peptides for reuse (Voges et al. 1999). The complex is ATP-dependent and responsible for 80-90% of cellular protein degradation (Thompson et al. 2008, Voges et al. 1999). While ubiquitination has long been associated with apoptosis, the process is also integral in cell-fate specification, transcription, and cell cycle progression.

CUL3 Ubiquitination

CUL3 is a gene located on chromosome 2 in the human genome, and the gene of interest for this study. It codes for the cullin 3 protein, which has a major role in polyubiquitination. Cullin 3 falls into the more common class of ubiquitin ligases, the cullins. The cullins are often referred to as CRLs, or cullin-RING ubiquitin ligases. Ubiquitination by way of CUL ligase is not exclusive to one protein, or even a family of proteins. It has many different substrates at many different stages of life. As a result, issues with CUL3 affects a cascade of different proteins and cellular processes. A few substrates of the ligase are well known, but many more are probably yet to be discovered (Andérica-Romero et al. 2013).

One known CUL3 ligand is the MEI1 protein involved in cell division. This particular protein is used in gamete formation primarily, as it signals the formation of a meiotic spindle. However, its creation and subsequent degradation is also required for the functional assembly of

a mitotic spindle (Pintard et al. 2004). Without CUL3 polyubiquitination and degradation, the mitotic spindle will form much more similarly to a meiotic spindle, where the spindle is formed on one side of the cell and uneven cleavage along the divisional plane occurs (Pintard et al. 2004). The result is two unequally sized daughter cells (Figure 3). Unfortunately, nearly all data surrounding inquiry into this protein comes from *Caenorhabditis elegans* zygotes, though there is a human homolog.

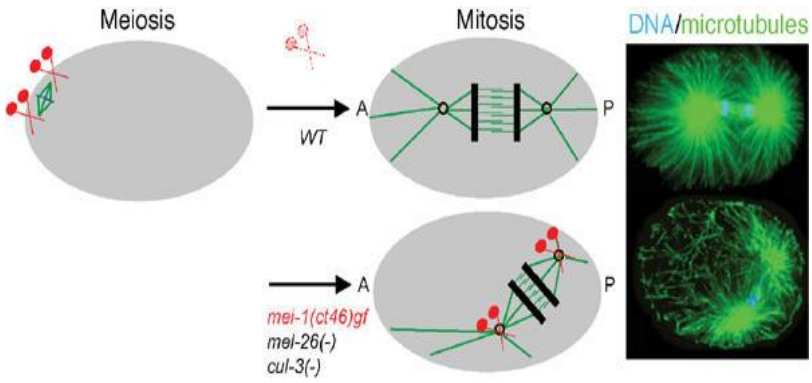

Figure 3. *Effects of CUL3 knockout on mitotic spindle formation*. (Pintard et al. 2004; Used with permissions from Wiley Online Library) CUL3 knockout eliminated MEI1 degradation from the cell cycle, allowing the mitotic spindle to form more similarly to the meiotic spindle.

CUL3 also targets Nrf2 (Nuclear-factor erythroid-derived-2-like 2), a transcription factor involved in the response to oxidative stress. During homeostasis, Nrf2 is constantly bound to KEAP1, an adapter protein that facilitates CUL3 targeting (Zhang et al. 2004A) Nrf2 is then ubiquitinated and degraded by the 26S proteasome. This process of rapid creation and degradation (turnover of about 20 minutes) continues until the cell undergoes oxidative stress, after which Nrf2 is allowed to aid in the transcription of many different proteins that respond to such a stress (Kobayashi et al. 2004; Zhang et al. 2004A). Overexpression of Nrf2 has been seen to aid in glioma resistance to the chemotherapy carmustine, though these results are only seen in neurological and immune cell cancers as these are the only cancers in which carmustine is used (Sukumari-Ramesh et al. 2015). In gastric cancers, Nrf2 expression has been directly correlated with cancer aggressiveness (Kawasaki et al. 2015).

Another target for CUL3 ligase proteasome degradation is the topoisomerase I protein, a complex that releases torsional stress on DNA during replication. Topoisomerase I (TOP1) is the main target of camptothecin (CPT)-type chemotherapies, two of which (topotecan and irinotecan) are currently FDA-approved. A knockout in CUL3 should increase the amount of TOP1 in the cell as there is no degradation machinery available to eliminate it. In fact, overexpression of CUL3 has been shown to induce resistance to CPT chemotherapies by way of down-regulation of TOP1, the target of CPTs (Zhang et al. 2004B, Beretta et al. 2013).

CUL3 has also been recently implicated in having a role in mitotic spindle stability and localization of chromosomes during anaphase. However, CUL3 does this through monoubiquitination (a process that has only two known CUL3 substrates) rather than polyubiquitination. This single ubiquitin is not enough to signal for proteasomal degradation, but instead simply alters protein function (Maerki et al. 2010). The target is Aurora B kinase, a component of the Chromosomal Passenger Complex (CPC). The CPC localizes to chromosomes at the beginning of mitosis and to the spindle microtubules as anaphase begins to ensure proper cytokinesis (Maerki et al. 2009, 2010). Monoubiquitination is critical for localization to the spindle. It has been suggested that ubiquitination allows Aurora B and the CPC to bind to the microtubules by way of an ubiquitin

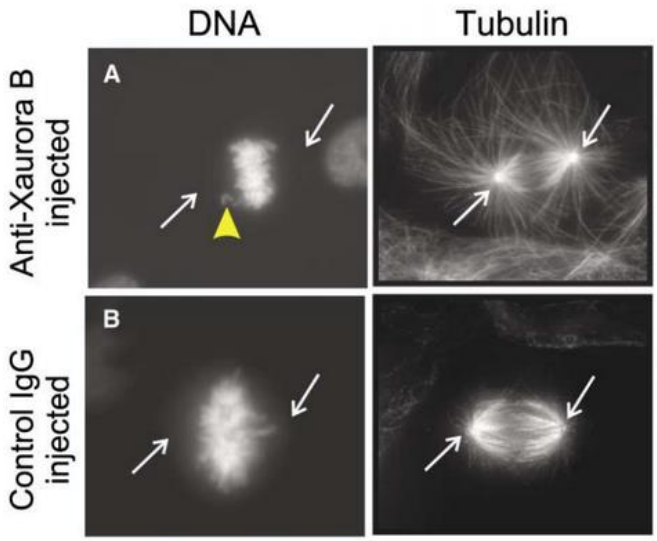

Figure 4. *Abnormal microtubule formation with Aurora B kinase inhibition*. (Kallio et al. 2002; Used with permissions from Elsevier) Anti-Aurora B antibody injection results in abnormal microtubule formation and mis-localized chromosomes. The yellow arrow shows at least one chromosome off of the divisional plane. The white arrows point to centrosome location.

binding domain (UBD) within one of the associated microtubule proteins (Maerki et al. 2010). Additionally, there is evidence that ubiquitination allows dissociation from mitotic chromosomes in the first place to allow secondary localization (Sumara et al. 2007). Localization is critical to properly cleave the cells, and failure to localize results in multinucleated cells (Maerki et al. 2009). Additionally, there is evidence that Aurora B inhibition results in more astral microtubule formation (deriving from the centrosome but not connecting to a kinetochore) and more fragile spindles in general (Kallio et al. 2002) (Figure 4). It should be noted that, unlike other substrates of CUL3 where knockout would result in their overexpression, CUL3 knockout effectively knocks out Aurora B function.

Notably, CUL3 has also been implicated in cyclin E degradation (Singer et al. 1999). Cyclin E is responsible for cell cycle control. Its attachment to Cdk2 (cyclin-dependent kinase) regulates cell cycle transitions (Hwang & Clurman 2005). The amount of free cyclin E during cell cycle transitions, which is often used as an indicator of Cdk2 activity, has best been characterized at the exit of G1 and the duration of S phase. Increased cyclin E expression is often the herald of the end of G1, often working in tandem with other mitogenic signals (Singer et al. 1999). Additionally, its abundance during S phase is inversely correlated with the duration of S phase (Hwang & Clurman 2005). CUL3 targets cyclin E in its unbound form, but if the ubiquitination process is interrupted, by CUL3 knockout or 26S proteasome inhibition, the cell cycle timing becomes disrupted. G1 is much shorter due to the abundance of cyclin E. The cells also spend more time in S phase than a normal cell (Singer et al. 1999, Hwang & Clurman 2005).

In addition to changes in duration of the cycle phases, there is also evidence that up-regulation of cyclin E results in more genetic instability. This implies that expression of cyclin E may increase the mutagenic and oncogenic properties of any given cell. It also gives some

interesting clinical applications as well. Many studies reviewed by Hwang and Clurman (2005) show a negative correlation between cyclin E expression and positive patient outcome, giving an effective diagnostic tool for evaluating cancer prognosis. Keyomarsi et al. (2002) found that patients with early stage breast cancers with high cyclin E expression all died within five years of diagnosis (12/12), while similar patients with low cyclin E expression all survived the five year mark (102/102). It has been shown, however, that cyclin E production is not directly correlated with speed of cancer growth in patients (Hwang & Clurman 2005).

What should also be noted is that CUL3 itself is regulated in many ways. Various BTB-domain (bricabrac-tramtrack-broad complex) Kelch-like proteins function as different adaptor proteins to target CUL3 to the specific protein of interest (seen in Figure 2). The BTB domain binds to the ligase while the Kelch domain binds to the substrate (Canning et al. 2013). Without these adapter proteins, CUL3 is unable to bind to target proteins and thus cannot catalyze ubiquitin attachment (Xu et al. 2003). For example, MEL26 is an adapter protein for MEI1. A *C. elegans* embryo with a MEL26 knockout expresses the same abnormal mitotic spindle expressed in a CUL3 knockout embryo (Pintard et al. 2004, Xu et al. 2003). When it comes to potential treatment avenues, individual BTB adaptor proteins could be targeted rather than CUL3 itself to ensure specific and effective treatment.

CUL3 is also regulated on larger scales by neddylation and deneddylation – attachment of Nedd8 to change the conformation of CUL3 and affect its function (Parry and Estelle 2004). While in reference to a CUL3 knockout neddylation patterns shouldn't affect much, overexpression of CUL3 would be more susceptible to Nedd8 alteration (see Figure 2).

CUL3's Role in Cancer

While CUL3 was implicated in murine lung cancer by Dr. Starr, the link of CUL3 to colorectal cancer is relatively unknown. The COSMIC (Catalogue of somatic mutations in cancer) database has one entry regarding colon cancer and CUL3, although it does have 34 listed entries that corroborate CUL3 as a general cancer driver gene (most of this information comes from unpublished data dumps, including the data regarding the gene's involvement in colon cancer).

An effective method of determining the role of a gene to cancer is to perform a knockout. This essentially mutates a gene to the point where the protein product is no longer functional. With a CUL3 knockout cell line, we may be able to evaluate CUL3's importance to cancer in a more meaningful way. A new method of performing a knockout (and the one used in this study) is the CRISPR/Cas9 system.

CRISPR/CAS9 AND GENE KNOCKOUT

The Discovery of CRISPR/Cas9

The CRISPR/Cas9 system was originally discovered in archaea and bacteria, which use the system as a defense mechanism against invading viral DNA and plasmids. It has been most extensively studied in the bacterial species *Streptococcus pyogenes*. Jinek et al. (2012) proposed its utilization as a biotechnological tool for DNA editing, as it is easily programmable and very specific.

In the single-cell organisms from which this system was derived, the viral DNA is integrated into the organism's own genome to target that same virus at the next instance of infection. Once the invading DNA enters the cell, it gets fragmented into protospacers which are

then integrated into the CRISPR (clustered regularly interspaced short palindromic repeats) array so that they come directly after the repeat sequence (Jinek et al. 2012). The cell now has multiple recognition sequences (spacers) targeting known invasive DNA, which can direct DNA silencing with Cas (CRISPR-associated) cutting enzymes (Figure 5). At the next instance of viral invasion, the Cas enzymes and the multiple spacer/repeat sequences, or crRNAs will be transcribed. The Cas enzymes, after translation, will align with the crRNA and the complex will meet the viral invader. If the crRNA sequence aligns with the viral DNA, the Cas enzymes will catalyze a blunt cut, inactivating the viral DNA and allowing its digestion by other nucleases (Jinek et al. 2012, Mali et al. 2013, Ran et al. 2013).

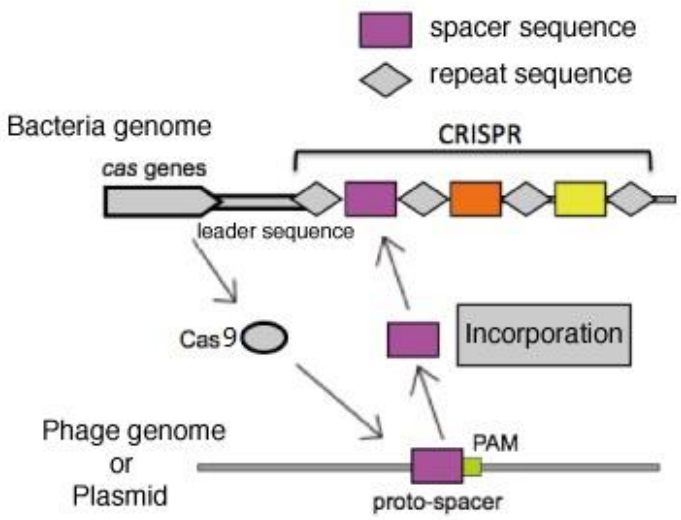

Figure 5. Diagram of CRISPR array and protospacer insertion in bacteria. (Adapted from Kyoto University Laboratory of Bacterial Infection) (Proto)spacers are integrated into a bacterial genome to directly follow the CRISPR repeat sequences.

While there are three types of CRISPR/Cas systems, the type II system has been the subject of further study with regards to biotechnological use. This is due to the fact that it requires only one Cas protein - specifically Cas9 - instead of a multi-Cas protein complex, like types I and III. In types I and III, the raw crRNA is altered by one Cas protein, and cleavage is caused by multiple other Cas proteins formed into a complex. Type II requires only one Cas enzyme (Cas9) because of the utilization of a second RNA, a trans-activating crRNA, or tracrRNA, that base pairs to the repeat sequence of the crRNA (Jinek et al. 2012).

The bacteria also avoid cleaving its own DNA by a very specific recognition system. It involves the protospacer's placement within the invasive DNA relative to a short specific nucleotide sequence, known as the PAM, or protospacer adjacent motif. For *S. pyogenes*, this sequence is NGG, placed three nucleotides upstream of the protospacer within the invasive DNA (Jinek et al. 2012).

The Use of CRISPR/Cas9 for Gene Knockout

The CRISPR/Cas9 system has become increasingly popular as a method of genome editing. It has all but replaced zinc-finger nucleases (ZFNs) and transcription activator-like effector nucleases (TALENs) as the go-to system for genome editing and gene knockout. These two systems have similar endonuclease activity to CRISPR/Cas9, but they take longer to make and are less effective overall. From start to finish, a CRISPR/Cas9 knockout can take only a month to complete (Ran et al. 2013). This study took two months.

To use the CRISPR/Cas9 system, certain changes needed to be made to the bacteria's system. The most obvious was to place the important pieces into a vector to place it into desired cells. Two options currently exist: one is plasmid vectors that are transfected into the organism of choice, and the other is a viral vector. Lentivirus is preferred here, as it can infect live hosts and dividing cells, ideal for animal modeling. Additionally the crRNA and tracrRNA portions were fused by a hairpin loop, making one long single guide RNA, or sgRNA, which only requires one template (Jinek et al. 2012; Hwang et al. 2013). The beauty of the CRISPR/Cas system is its genetic brevity, making vector transfection rather simple.

Lastly, targeting to the gene of interest is needed. This involves finding an approximately 20 bp section (protospacer) within the mRNA of the desired gene that is three base pairs downstream of a specific PAM sequence (Figure 6). The number of base pairs between the

protospacer and the PAM and the exact PAM sequence is dependent on the organism of derivation of the sgRNA and the Cas9 enzyme, as they vary from species to species (Jinek et al. 2012). After the target sequence is chosen, this sequence is added to the 5' end of the sgRNA template to create the spacer. The spacer is the only portion of the entire CRISPR/Cas9 complex that changes from target to target (Jinek et al. 2012; Mail et al. 2013). Depending on the target cells, whether they are human or mouse or other, the Cas9 enzyme coding sequence is often altered to optimize for the codons commonly used in the organism of interest. Additionally, human (or other organism's) promoters are used at the beginning of the Cas9 and the sgRNA sequences to ensure constitutive expression once within the cells. For example the human U6 polymerase III promoter is commonly used in front of the sgRNA when transfecting human cell lines *in vitro* (Mali et al. 2013).

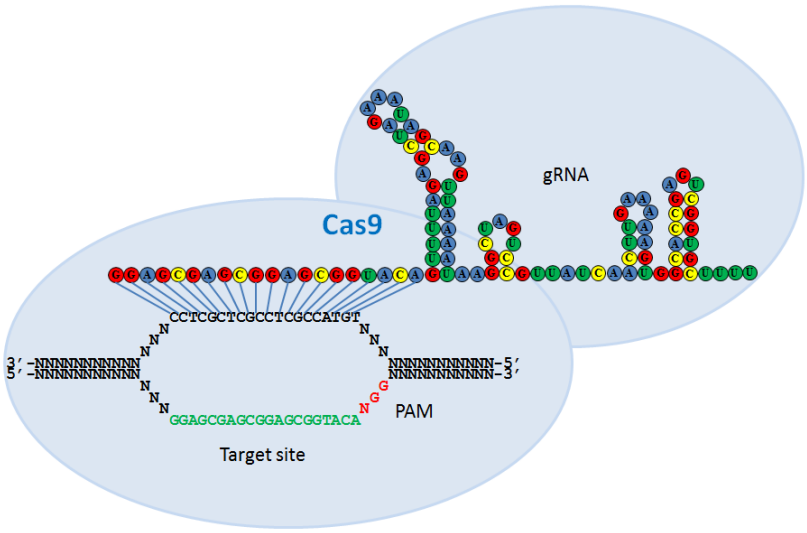

Figure 6. *Configuration of sgRNA and Cas9 with genomic DNA*. (Hwang et al. 2013; Used with permissions from the Nature Publishing Group) Above shows the structure of the sgRNA and how it targets within the genome. Note the PAM sequence NGG directly downstream of the target site.

Once the cells have been transfected, either by viral vector or plasmid (as was used in this study), the system uses the cell's own internal machinery to transcribe the Cas9 enzyme and the sgRNA, aided by the humanized promoters. The Cas9 enzyme associates with the crRNA and tracrRNA domains of the sgRNA. The Cas/sgRNA complex then aligns with the protospacer and the PAM sequence while holding apart the two strands of the target DNA. The Cas9 enzyme

then catalyzes cleavage of each individual strand of the DNA. Hopefully, this cleavage will result in a mutation when rejoined by non-homologous end joining (NHEJ) (Ran et al. 2013). NHEJ is used when both DNA strands are cut and a DNA template for the region is unavailable. It involves the recruitment of various capping proteins that bring the two ends together and a ligase (ligase IV) to reconnect the strands. It often results in frameshift mutation, as some nucleotides can be lost during DNA cleavage or inserted in the repair process (van Gent & van der Burg 2007).

If mutation does not occur during DNA repair, the system will repeat the process, as long as the spacer can still recognize the protospacer (Hsu et al. 2013). This process also ensures DNA mutation as long as the templates for both the Cas9 enzyme and the sgRNA plasmids were successfully transfected into the cell.

Off-Target Effects

While the system is specific and efficient, there is also the possibility of off-target effects, as there are with any nuclease. The number of off-target sites and the frequency of off-target cutting is dependent on the sgRNA sequence chosen. Obviously if the target sequence exists in more than one place in the genome, Cas9 with catalyze cleavage at both sites about equally. Ran et al. (2013) found that some level of mismatch is allowed in sgRNA base pairing with its target. For the most part, only three or less mismatches in the 20 bp sequence, or 85% or more sequence homology, is tolerated. Additionally, mismatches are more tolerated at the 3’ end of the sequence. The frequency of mismatch base-pairing is also dependent on the concentration of Cas9 and sgRNA transfected into the cells, as well as their ratios. The frequency of off-target cutting increases as the concentration of Cas9 plasmid dosage at initial transfection increases (Hsu et al. 2013).

The easiest way to prevent off-target effects is to carefully select the sgRNA sequence. Certain design databases such as ZiFiT (Sander et al. 2010) and the CRISPR Design Tool (http://tools.genome-engineering.org) will give the most likely off-target sites with every potential target sequence. However, they are still possible even with the greatest precautions and should therefore be analyzed in all uses of CRISPR/Cas9.

PURPOSE OF STUDY

CUL3 has been shown to be an important driver gene in lung tumorigenesis in mice. Due to the implications that this gene is a general cancer driver gene, CUL3 is likely also important in human CRC development. CUL3 ligase has many different known substrates – some of which may have effects on cell health and cancer proliferation. We have attempted to evaluate the importance of CUL3 to human CRC using CRISPR/Cas9 based CUL3 knockout in the HCT-116 human colorectal cancer cell.

METHODS

Cell Culture

HCT-116 cells were cultured at 37° C and 5% CO_2 in DMEM (Dulbecco's Modified Eagle Medium) (Gibco, Grand Island NY), supplemented with 1% L-Glutamine (Gibco, Grand Island NY), 1% Penicillin/Streptomycin/Fungizone (PSF) (Gibco, Grand Island NY), 2.5% HEPES buffer (Gibco, Grand Island NY), and 10% Fetal Bovine Serum (FBS). Cells were stored frozen in FBS containing 10% DMSO (Dimethyl sulfoxide) (Sigma-Aldrich, St. Louis MO) and cryopreserved in liquid nitrogen until needed. When cells were passed, they were first removed from culture flasks by treatment with 0.5% Trypsin-EDTA (Gibco, Grand Island NY) for 10 minutes. After trypsin neutralization, they were diluted 1:20 in their new flask, unless an abnormal (slowed) growth phenotype was seen, in which case they were passed 1:10.

Puromycin Assay

The HCT-116 cells were plated at a 1:10 dilution in a 96-well plate and allowed to grow up for three days. After the cells had reached 80-90% confluence, the media of some wells was removed and replaced with puromycin media at various concentrations of puromycin: 10 ug/mL, 5 ug/mL, 2.5 ug/mL, 1.25 ug/mL, .625 ug/mL and 0 ug/mL. Four replicates of each concentration were created in the plate. Every 24 hours after the initial media replacement, one well of each concentration was removed and counted by trypan blue exclusion. At the end of three days, the minimum concentration that produced complete death was chosen. In this experiment, 1 ug/mL of puromycin was chosen for subsequent selection steps. This concentration is consistent with the 1 ug/mL concentration used by Dr. Starr at the University of Minnesota for this cell line.

Lipofectamine Assay

HCT-116 cells were plated in a 24-well plate and allowed to grow until at 60-70% confluence, or about two days. After confluence had been achieved, the cells were transfected with two plasmids: the Piggy-BAC puromycin resistance plasmid and the pB7 transposase plasmid. To determine the ideal concentration of the transfection chemical, Lipofectamine (Invitrogen, Carlsbad CA), the cells were transfected with varying concentrations (1uL, 1.5 uL, 2uL, and 2.5 uL/mL media) of Lipofectamine. Each well was given .25 mg of each plasmid per mL. Prior to transfection, the plasmids and Lipofectamine incubated in OptiMEM media for 5 minutes to ensure full coating of the plasmids in the Lipofectamine. The Lipofectamine-plasmid complex was then added to the media of 2 wells (per concentration) of the 24-well plate (see Appendix 5). After the addition of the Lipofectamine-plasmid complex, the cells were allowed to recuperate and grow for 24 hours. This also allowed enough time for the cells to take up the antibiotic resistance plasmids and become puromycin-resistant. After this 24 hour period, the media of the transfected cells was replaced with media containing puromycin at the predetermined 1 ug/mL concentration. The cells were allowed to sit in the puromycin for four days undisturbed. After this 4 day period, the cells were analyzed for overall confluency. Optimal Lipofectamine dilution was chosen based on which concentration produced the highest number of transfected (puromycin resistant) cells.

Confluency Assay

HCT-116 cells were plated in 4-well increments at varying concentrations ranging from 100-5000 cells per well. They were allowed to grow up for four days. After this time, overall confluency was recorded. The lowest concentration that resulted in an average of approximately

90% confluency was determined to be optimum. For HCT-116, this was approximately 2500 cells per well.

U6-sgRNA Plasmid Design

Plasmid design was performed by Dr. Goldberg's lab in the summer of 2013. The empty U6-sgRNA plasmids (without a target sequence introduced) were obtained from Dr. Starr at the University of Minnesota. Inverse primer design was performed using the ZiFiT computer program, which locates multiple target sequences within the target gene that also has the PAM sequence directly after the target DNA (Sander et al. 2010). In this study, the CRISPR/Cas9 system was derived from *S. pyogenes*, making the PAM sequence NGG. The plasmids were created using Inverse PCR and frozen in nuclease-free water at -20° C until use in 2014.

CRISPR/Cas9 Knockout

HCT-116 cells were plated in a 24-well plate and allowed to grow two days until they reached 60-70% confluency. After this time, the cells were transfected using the predetermined Lipofectamine concentration. Four plasmids were placed in each well: the Piggy-BAC transposon with puromycin resistance, the pB7 transposase plasmid, the Cas9 endonuclease plasmid, and the pU6 RNA guide sequence. Three different U6 guide sequences were created previously to target the CUL3 gene. Two wells of the 24-well plate were transfected for each pU6 plasmid. The Piggy-BAC and pB7 were still at 0.25 ug per well, but the Cas9 and the pU6 were added at 1 ug per well in an effort to ensure that every colony that received antibiotic resistance would also likely have the knockout. After Lipofectamine-plasmid complex incubation, the wells were transfected and allowed to grow up an additional 24 hours before subcloning.

Subcloning

24 hours after transfection, the transfected cells were removed from the 24-well plate and replated in 96-wells in 1 ug/mL puromycin media at low density (2000-3000 cells per well), determined by the confluency assay. After 8 days of incubation with puromycin media, clonal colonies were selected by locating wells with a single colony that had arisen from a single cell. Over the next month, selected cell lines were removed from their wells when appropriate (60-70% confluency) using 0.5% Trypsin-EDTA incubated for 5-15 minutes. They were placed into a larger culture container until they could maintain normal growth in a 25 mL culture flask. At this point, cells were partitioned off for DNA extraction and freezing.

Imaging

All images were captured with an inverted light microscope set at 100x connected to an iPhone 5 (2013). Images were adjusted to improve clarity by Windows Photos (2014).

DNA Extraction

DNA extraction was performed with the Promega Wizard Genomic DNA Purification Kit (Madison, WI). Resulting DNA purity and concentration was determined with a Nanodrop 2000.

Primer Design and PCR

Primers were designed by hand using the genomic CUL3 DNA sequence from NCBI Blast. Primer alignment was confirmed using PrimerQuest and IDT (Integrated DNA Technologies) Primer Design. Primers were obtained from IDT (Coralville IA) as standard desalted oligos (sequences in Appendix 1).

PCR was performed using Gotaq Green Master Mix (Promega, Madison WI), the previously mentioned primers and extracted DNA to amplify the regions of intended knockout for sequencing as per Gotaq protocols (see Appendix 3). PCR was performed using an

Eppendorf Mastercycler Nexus Gradient Thermal Cycler according to manufacturer suggestions using the program outlined in Appendix 2.

Confirmation of successful PCR was done by gel electrophoresis. PCR product was run on a 1% agarose gel using a BioRad MiniSub® Cell GT Cell horizontal gel box and compared to a Bioline (Boston MA) 50 bp ladder. The gel was imaged with a BioRad GelDoc XR+ UV transilluminator to ascertain appropriate band length and PCR product amount.

PCR product was purified using the Promega SV Gel and PCR Clean-Up System (Madison WI). Resultant products were maintained in the provided EB buffer before sequencing.

Sequencing and Confirming Knockout

Sequencing of PCR products was performed by Functional Biosciences (Madison, WI). The sequencing results of all cell lines created using the P1 sgRNA guide plasmid were aligned using ClustalW to look for genetic inconsistencies between the Ctrl (parental) sequence and the various transfected cell lines. Any nucleotide differences within 10 bp of the supposed target site from the parental HCT-116 DNA sequence was considered to be a confirmed knockout.

MTS Assay

HCT-116 cells were plated at low density, previously determined by the confluency assay, in 12 wells of a 96-well plate, placed in 2 rows of 6 wells. Four plates per cell line were created to take data over a four day span. Each day, one plate was used for analysis. 6 of the 12 wells per cell line had 20 uL of Promega AQueous ONE CellTiter MTS Liquid (Madison, WI) added, and all used plates were placed back into the incubator for four hours to allow colorimetric development. The 12 wells were measured with a plate reader at both 490 nm and 650 nm. This process was repeated for four straight days to determine changes in metabolic rate over time.

Off-Target Sites

Potential sites of off-target cutting for Cas9 construct #1 were determined using an NCBI Blast search for the primer and PAM sequence. The PAM sequence used was both NGG and NAG, as Hsu et al. found that both PAMs can be recognized for off-target cutting (2013). Any result below 80% homology was also excluded based on Hsu et al.'s findings.

RESULTS

Various Experimental Assays

As the mutant cells should carry puromycin resistance after transfection, an ideal concentration of puromycin, one that would allow complete death of all non-resistant cells (e.g. non-transfected cells) in 4 days, with the lowest concentration possible to avoid damaging the mutant cells, was required. This was determined by exposing wells of HCT 116 to varying concentrations of puromycin and recording the percent viability daily for three days. As shown, a concentration of 1.25 ug/mL or above of puromycin is ideal to see total death after three days (Figure 7). This study required four or more days in puromycin, though the data was taken over three days. As 1.25 ug/mL was effective after three days, and 0.625 ug/mL showed little-to-no change after three days, our results were in the range of the Starr lab's experimentally determined value of 1 ug/mL, which was used in further experiments.

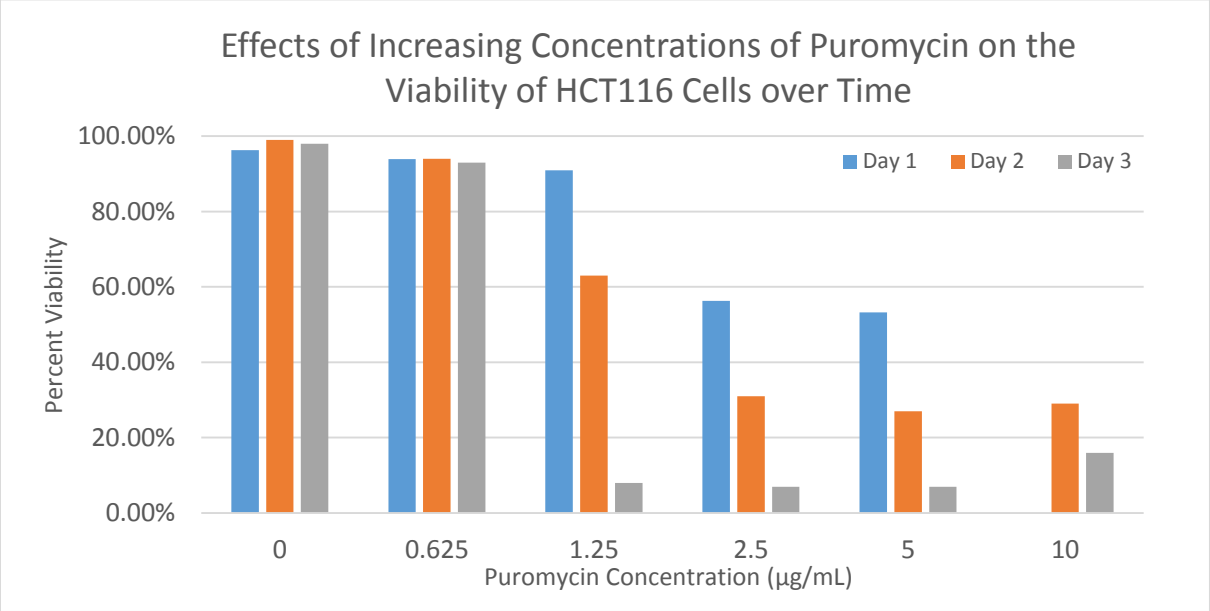

Figure 7. *Percent Viability of Cells based on Puromycin Concentration*. Percent viability was determined over 3 days by trypan blue exclusion. A concentration that produced total death after four days is ideal.

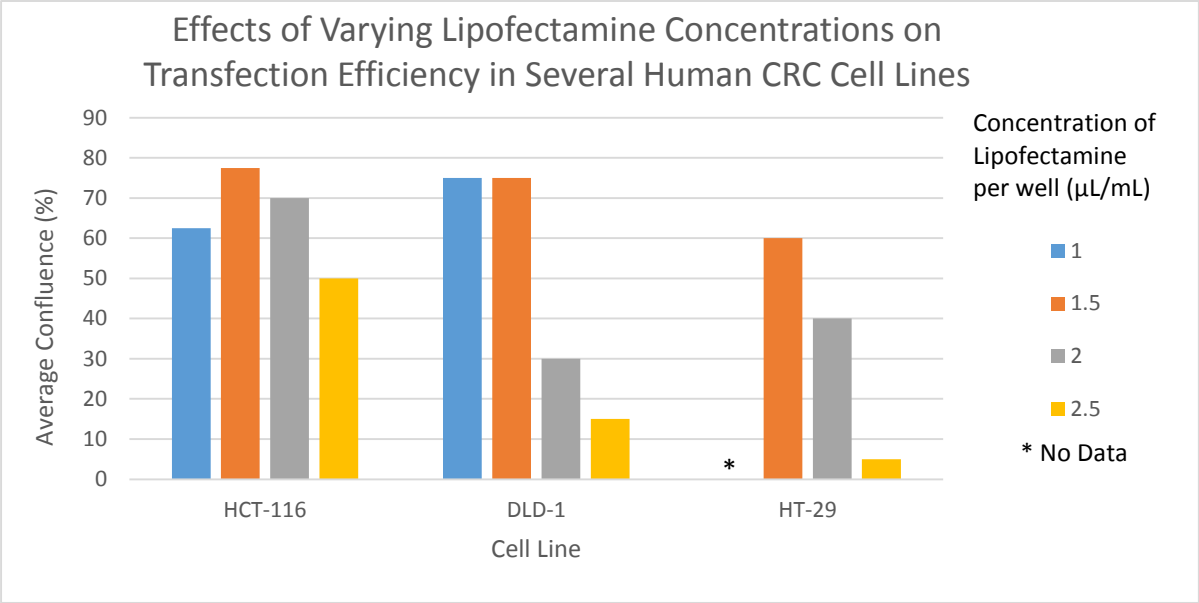

Figure 8. *Lipofectamine Assay*. Three colorectal cancer cell lines were transfected with puromycin antibiotic resistance plasmids with varying concentrations of Lipofectamine. After four days of treatment with puromycin, the confluency of the treated wells was determined.

The ideal concentration of lipofectamine, the chemical used in transfection, was determined by transfecting CRC cells at varying concentrations of lipofectamine and the puromycin resistance plasmids, and then subsequently incubated in the previously determined puromycin concentration. A concentration too low would not allow all transfection possible and a concentration too high could prove toxic to the cell. This assay was performed not only with HCT-116, the cell line used in this study, but with DLD-1 and HT-29 as well, two other CRC cell lines that, in the future, may also be mutated and evaluated (Figure 8). As shown, a lipofectamine concentration of 1.5 uL/mL media was determined to be ideal for all three cell lines. For HCT-116, Figure 9 shows the raw confluency and number of

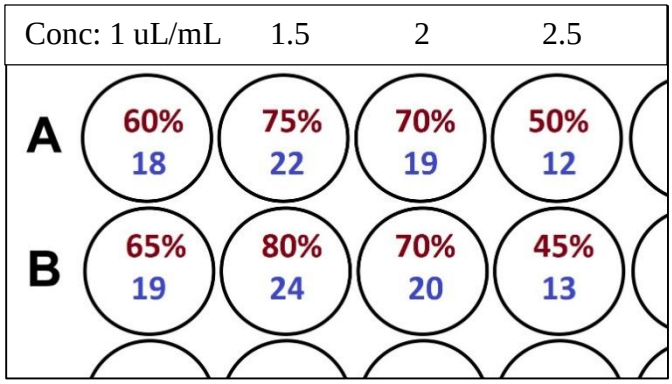

Figure 9. *HCT-116 Lipofectamine Assay results*. Results were taken on Day 4 of the assay. In red, confluency of the well is shown. In blue, the number of individual colonies is shown.

colonies data four days post transfection and puromycin treatment.

To ensure the cells were plated at a low enough concentration to achieve the desired one-living-cell-per-well ideally needed to create individual clonal cell lines, a confluency assay was performed. The goal was to determine the concentration of cells that would take four days to achieve a confluency of 85-90% (Results in Figure 10). Cells were plated at initial concentrations varying from 100-5000 cells per well in a 96-well plate. A 96-well plate was used because that was the plate to be used to start our clonal colonies. After four days of growth at varying concentrations, the ideal concentration chosen was between 2000 to 3000 cells. Previous plating attempts showed that a concentration closer to 3000 cells/well was too concentrated to produce single clonal colonies in one well at a high enough frequency, so for our purposes, transfected cells were plated at an initial concentration closer to 2000 cells/well. Anecdotally, nearly all wells found to have any living cells contained single clonal colonies, with only a handful of wells containing two or three colonies. The 41 cell lines obtained were from 6 plates (or 576 total wells), and no single clonal colony was left out.

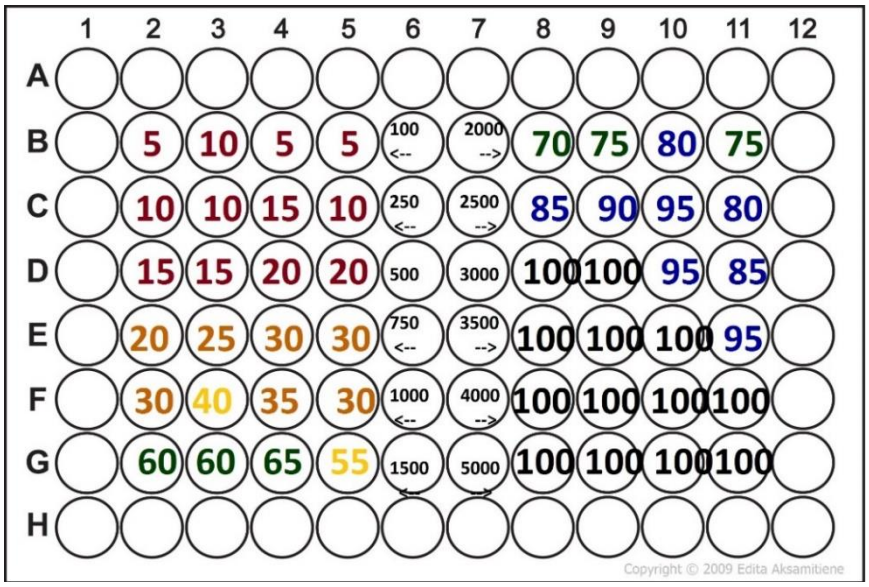

Figure 8. *Confluency assay results of HCT-116*. Cells were plated at varying concentrations (100-5000 cells/well) and grown for four days. The above results show the approximate confluency in that time. For HCT-116, approximately 2500 (or 2000-3000) cells per well achieved an ideal confluency (approximately 85-90%) after four days.

Observational Data

Cell Line	Growth Speed (approximate)	Abnormal Morphology?	Extra-Large Cells	Abnormal Adherance
Parental	Fast	No		
1MY1	Medium	Yes		*
1MY2	Medium	Yes		*
1SY1	Slow	Yes	+	
1SY2	Slow	Yes	+	
1SY5	Slow	Yes	+	
1SSY2	Super Slow	Yes	+	

Table 1. *Parental and confirmed knockout cell line observational data*. Cell lines are categorized at various growth speeds and whether or not they exhibited abnormal morphology.

10 days post-transfection and puromycin treatment, individual clonal cell lines were selected and evaluated. Speed of growth was ascertained by approximate colony size after 10 days and categorized into four categories: Fast, Medium, Slow, and Super Slow. Those cell lines categorized as Fast and Medium were transferred to a 24-well plate to allow further growth. Slow speed cell lines were transferred 7 days later (17 days post-transfection), and Super Slow speed cell lines were transferred 2 days after that (19 days post-transfection).

Once the cells were transferred to culture flasks, the growth speed as a measure of frequency of passage was taken. The parental cell line (with all cell lines normalized to its rate of passage) was seen to have a passage rate of half or less than the passage rate of any knockout

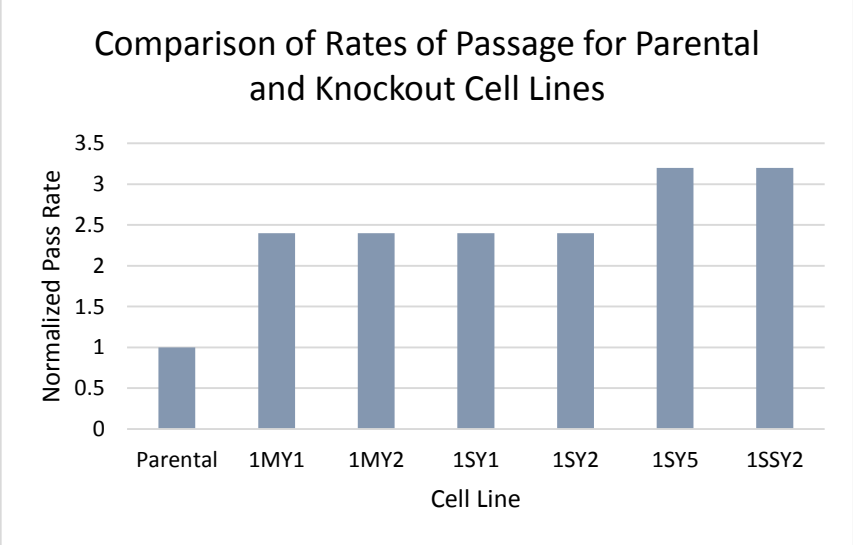

Figure 9. *Comparison of passage rates for parental and knockout cell lines*. The cells were passed at a frequency relative to their growth speed and the rate at which they ran out of culture flask surface space. The fewer days between passes, the faster the cells grow. All data is normalized to the ratio of passage.

cell line, which indicated that it grew at twice (or more) the speed of the knockouts (Figure 11).

Further evaluation while the cells continued growing was done based on approximate size of cells and adherence to the cell culture surfaces. Of the 14 cell lines categorized as Fast (within all three sgRNA constructs), no cell line exhibited any abnormal morphology. These cell lines

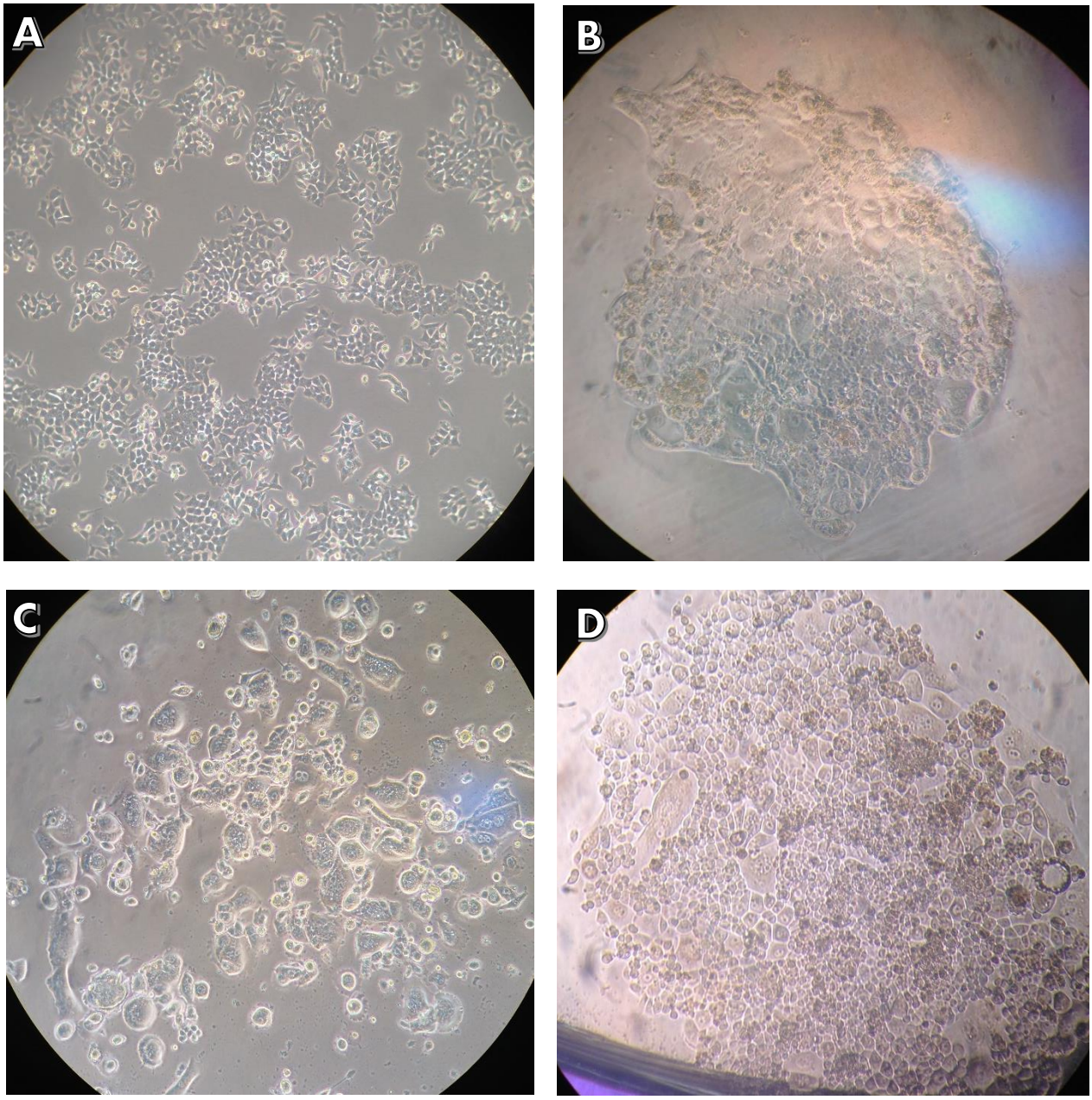

Figure 10. *Phenotypic differences between cell lines.* HCT-116 (A) shows parental cell line growth, 1MY2 (B) shows abnormal cell flask adherence, and 1SY5 (C) and 1SY1 (D) display abnormally sized cells. All images were taken at 100x.

also grew at the approximate speed of the parental cell line in all culture container types (96-well, 24-well, 6-well, and flask). 8 of 11 Medium speed cell lines exhibited abnormal phenotypes, with 7 of 8 exhibiting abnormal adherence (5 less adhered, 2 more adhered), and 3 of 8 exhibiting extra-large cells among the normal sized cells (as compared to the parental cell line) (Examples in Figure 12). The 13 cell lines exhibiting Slow growth speed all exhibited some sort of abnormal phenotype. 10 of the 13 exhibited extra-large cell sizes and 6 of the 13 demonstrate differing surface adherence (3 less and 3 more adhered). All 4 Super Slow cell lines exhibited expanded cell size. It should be noted that, depending on the degree of largeness seen in the cells, and the percentage of cells with this affliction could potentially interfere with visual flask adherence observations, due to sheer inexperience with this type of cell.

Determining Knockout

PCR program and primers were confirmed to work by gel electrophoresis (Figure 13). The gel also demonstrated that the PCR product was ample for sequencing (based on band brightness) and relatively pure.

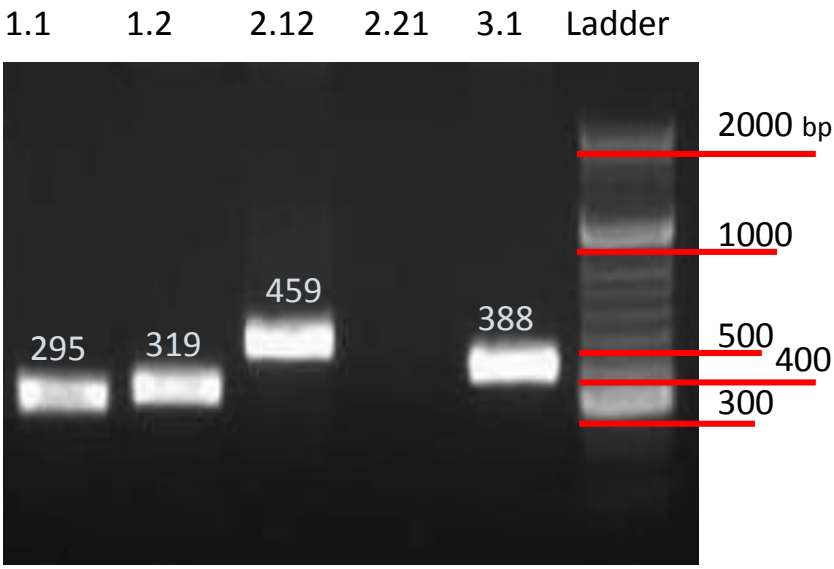

Figure 11. *Confirmation of desired PCR product*. Primers used to amplify the region of intended knockout were used on genomic HCT-116 DNA to ensure ample PCR product at the intended length in base pairs. Assumed length is above each band, and ladder band values are underlined in red. Primer sets (above their respective lanes) can be found in Appendix 1.

Knockout was suspected in all cells containing an abnormal phenotype and not suspected in cell lines that did not exhibit the abnormal phenotype. As a result, only one cell line in the Fast

growth category was evaluated for knockout. As stated, PCR was only performed in the area of attempted knockout – three different areas for the three different sgRNA constructs. As knockout was only able to be confirmed in six cell lines, all transfected with sgRNA construct #1, those results are shown, compared to the one Fast cell line, the parental cell line, and the one cell line that does not contain a knockout, 1SSY1. Knockout was obtained in all confirmed cell lines by way of frameshift, or indel, mutation. All cell lines show some sort of insert, and three of the six

```
Cell Line    Sequence
Ctrl1        GAGAACGTCTACAATTT----------GGGATTAATTATTTTTCGAGATCAAGTTGTACG
1SSY1        GAGAACGTCTACAATTT----------GGGATTAATTATTTTTCGAGATCAAGTTGTACG
1SY1         GAGAACGTCTACAATTTT---------GGGATTAATTATTTT-CGAGATCAAGTTGTACG
1SY2         GAGAACGTCTTTT--------------GGGATTAATTATTTTTCGAGATCAAGTTGTACG
1SY5         GAGAACGTCTACAACATCAAAACATCAAACGTTAATTATTTTTCGAGATCAAGTTGTACG
1SSY2        GAGAACGTCTACAATTTTT--------GGGATTAATTATTTTTCGAGATCAAGTTGTACG
1MY1         GAGAACGTCTACAAAATTT--------GGGATTAATTATTTTTCGAGATCAAGTTGTACG
1MY2         GAgAAcgtcTACAATTTTTT-------GGGATTAATTATTTTTCGAGATCAAGTTGTACG
1FN1         GAGAACGTCTACAATTT-------------------------------------------
             **********
```

Figure 12. *Alignment of sequencing results of confirmed knockouts*. Six cell lines (1SY1, 1SY2, 1SY5, 1SSY2, 1MY1, 1MY2) have confirmed knockouts by way of frameshift mutation (highlighted in blue), 1SSY1 can be confirmed to have no knockout at this location, and knockout in 1FN1 is unable to be determined.

also show some sort of deletion (Figure 14).

Due to frameshift mutation in all cell lines except 1MY2, the protein product derived from the mutant CUL3 mRNA is expected to be largely inaccurate, potentially creating a premature STOP codon and translating all amino acids after the site of mutation in the wrong open reading frame. 1MY2 would result in the addition of an amino acid to the sequence, which could affect protein folding or interactions of the ligase with other proteins.

Changes in Metabolic Activity

MTS is an altered, more accurate form of the MTT assay (both named for the type of tetrazolium salt used). This assay measures metabolic activity, and therefore cell growth and survival, by the conversion of tetrazolium salt to formazan. This change is catalyzed by the

mitochondrial enzyme succinate dehydrogenase, which cleaves the salt to form formazan. The cleavage results in a color change that is then read by a spectrophotometer (Buttke et al. 1993, Denizot and Lang 1986).

Preliminary data (resulting from one run of the assay) suggests that CUL3 knockout has resulted in an increase in metabolic activity (Figure 15). All cell lines with a confirmed knockout had significantly higher formazan output than the parental cell line for the first two days. By the fourth day, the parental cell line had caught up to the knockouts, indicating that all cell lines may have tapered off in metabolic activity increase. This is usually the result of reaching spatial constraints and commonly seen in the parental cell line.

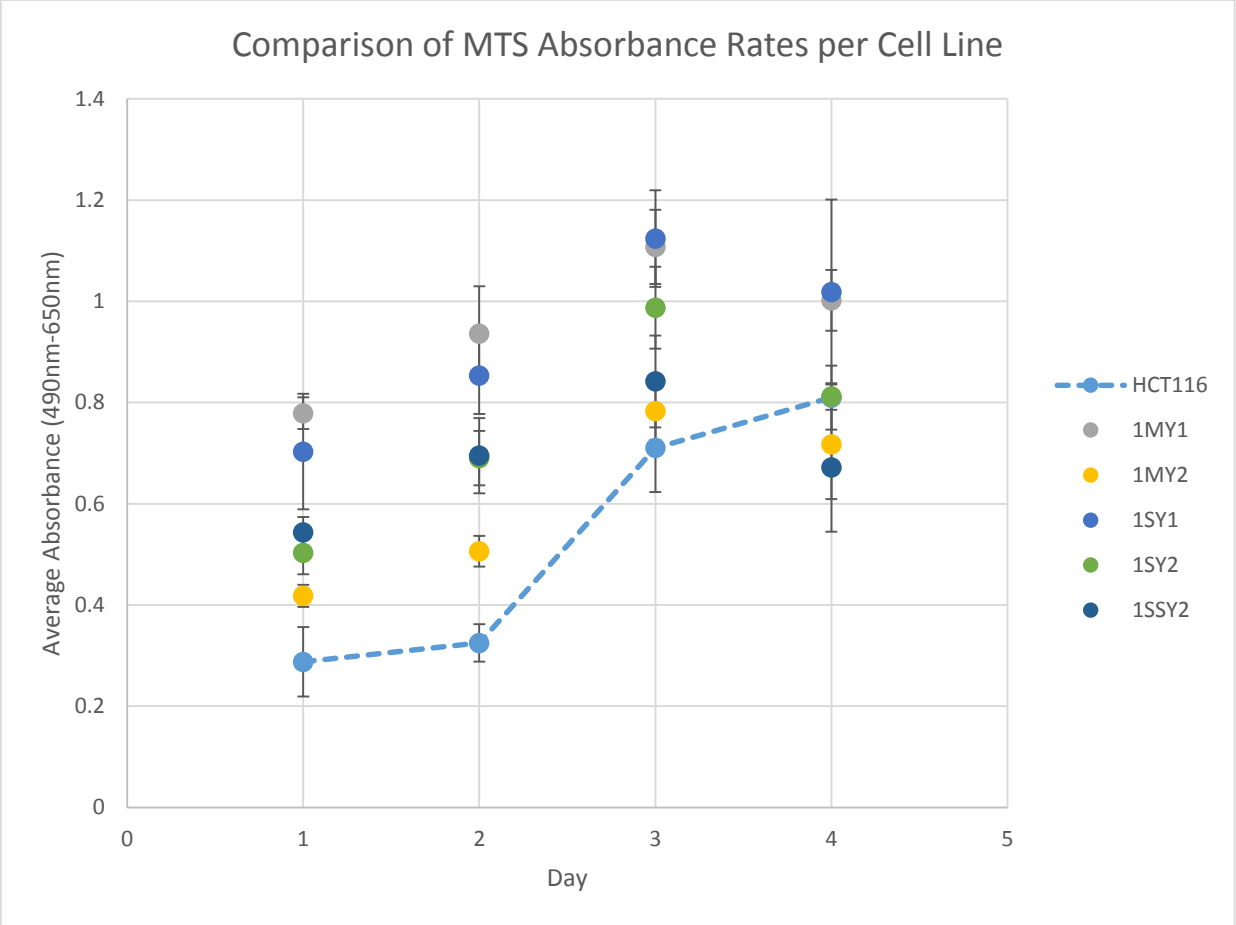

Figure 13. *Comparison of the MTS Absorbances of Various Cell Lines*. The (490nm – 650nm) absorbances after treatment with MTS CellTiter liquid of each knockout cell line (sans 1SY5) are compared day by day. The control (HCT 116) is outlined with a dotted line.

Off-Target Effects

An NCBI Blast search for the target sequence and PAM (both NGG and NAG) was performed to locate sites within the human genome that may be targets of off-target cutting. The Blast search resulted in five potential off-target cut sites in actual genes. Two other sites were found in non-coding regions of the genome (Figure 16). Of the five potentially deleterious off-target sites, only one had homology of over 90% to the original target sequence. Two had over 85% homology, but both had the NAG PAM, indicating that they might be less likely to bind than a NGG counterpart.

Cell Line	Sequence	Homology
CUL3	TGGAGAACGTCTACAATTTNGG	100%
NC1	-GGAGAATGTCTACAATTTGGG	90.9%
RAVER2	---AGAACGTCTTCAATTTGGG	81.8%
PEX1	TGGAGAACTTCTACATTTTTGG	90.9%
NC2	--GAGAACTTCTAAAATTTTGG	81.8%
LRPPRC	--GAGAATGTCTAAAATTTTGG	81.8%
BBX	TGGACAACGTCTAAAATTTGAG	86.4%
FOX1	TGGAGAAAGTCTACAGTTTAAG	86.4%
	* ** ***:.* *** .*	

Figure 14. *Possible Off-Target Effects*. The potential off target sequences compared to the P1 CUL3 target sequence used in the sgRNA CRISPR. NC1 & 2 are non-coding regions, RAVER2 is Ribonucleotide PTB-binding 2, PEX1 is Peroxisomal biogenesis factor 1, LRPPRC is Leucine-rich PPR motif containing protein, BBX is an HMG box transcription factor, and FOX1 is Forkhead box protein 1.

DISCUSSION

EXPERIMENTAL FINDINGS

Morphological Changes

In every cell line with a confirmed knockout, morphological changes were seen. While the specific changes vary from cell line to cell line, the majority of cell lines with confirmed knockout exhibit a phenotype that would be expected of a CUL3 knockout.

The morphology seen could be due to CUL3's effects on monoubiquitination of Aurora B kinase, an enzyme involved in mitotic spindle stability and cytokinesis. Because of the function of monoubiquitination as a modulator of protein function and localization (as opposed to degradation targeted by polyubiquitination), a CUL3 knockout essentially results in knockout of Aurora B's secondary function and localization (Maerki et al. 2010, Sumara et al. 2007). Sumara et al.'s results using RNAi to inhibit CUL3 translation best exemplifies visually the resultant multinucleation and inhibited cytokinesis, seen in Fig. 17 (2007). The mechanism by which this is occurring is elucidated by Maerki et al. (2009, 2010), where they posit a role for Aurora B monoubiquitination in aligning chromosomes to the divisional plane. Aurora B degradation, similar to inactivation, has been shown to result in faulty cytokinesis and multinucleation. Additionally, there is evidence that inhibition of normal Aurora

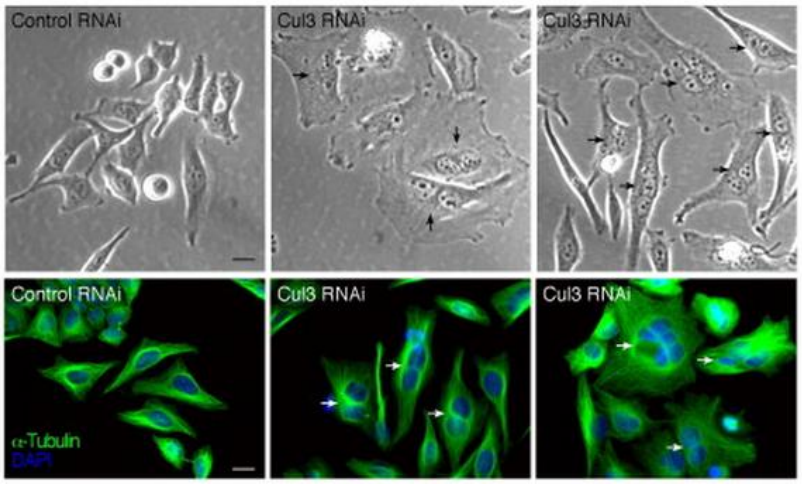

Figure 15. *Multinucleation due to CUL3 knockdown.* (Sumara et al. 2007; Used with permissions from Elsevier) RNAi that inhibits CUL3 function results in multinucleated cells due to interference with normal Aurora B function.

B activity results in excess microtubule formation, increasing especially astrally (from the centrosome but not connecting to a kinetochore) (Figure 4) (Kallio et al. 2002).

Because multinucleation and failed cytokinesis halts the cell cycle, Aurora B inhibition could also be seen to slow the overall growth rate of a cell culture, which may explain the need for less frequent passage in the knockout cell lines. We expect that if Aurora B was completely inhibited, no cytokinsese would occur and the cells would not survive. However, though Aurora B monoubiquitination is critical for cytokinesis and its inhibition, in all literature reviewed, it does not seem to effect all cells in the culture identically. In this way, CUL3 knockout to disable Aurora B monoubiquitination is more similar to a knockdown of Aurora B monoubiquitination. This means that Aurora B function is severely inhibited, but not completely gone, allowing some cells to survive and reproduce.

Metabolic Activity

The MTS assay used in this study is traditionally used as a method of ascertaining proliferation of cells. Changes in metabolic activity can easily be correlated with changes in cell growth in culture. This is assuming a relatively homogenized culture, with cells with equivalent ATP requirements and mitochondrial output. However, if a mutation causes abnormal metabolic activity, this assay no longer accurately measures the number and rate of cell proliferation.

Due to time constraints, the MTS assay had only one trial, with six individual wells measured per cell line. Given that only one assay was performed, this assay will need to be replicated to determine if the effects seen are reproducible. The trends here indicate that metabolic activity increases in knockout cell lines, but one trial gives the conclusions drawn little confidence. Therefore the first step before any concrete conclusions are drawn would be to rerun the assay to the point where statistics can be run.

None of the afore-mentioned substrates of CUL3 give an ideal explanation for why CUL3 knockout cells would suddenly have higher metabolic activity. Likely, if the effects are due to the knockout, the substrate responsible for increased metabolic activity has yet to be discovered. There is also the possibility that the abnormal metabolic activity is due to off-target Cas9 cutting.

Off-Target Effects

As previously stated, occasional off-target effects are unavoidable. Sequencing data of the 1SSY1 cell line shows that no knockout occurred at the expected site. However, this cell line still exhibited abnormal morphology and a substantially slowed growth rate (anecdotally). This cell line is the most likely candidate for off-target cleavage. Of the seven off-target sites identified in Figure 16, only four fit the criteria outlined by Ran et al. (2013), which includes over 85% homology with the mutations at least 4 bp away from the PAM sequence. Only one is within a non-coding region of DNA. The other three, PEX1, BBX, and FOX1, are the most likely sites of off-target cutting, with priority to PEX1, as it retains the NGG PAM sequence and has a higher percent homology (91% v. 86%) to the target sequence. Further study is needed to determine whether or not these off-target sites are responsible for the abnormal morphology seen in 1SSY1, and potentially other cell lines.

PERFECTING THE CUL3 KNOCKOUT

Alterations to the Current Approach

The CRISPR/Cas9 system, as described in the methods portion, produced six successful KO-CUL3 cell lines. However, since six out of 41 total cell lines is a 14% success rate, the knockout efficiency could be increased with alterations to the approach.

Another option would be to introduce multiple protospacers within the gene of interest per transfection in hopes that, if one target does not work, another may do better. In the archaea and bacteria from which this system is derived, multiple protospacers targeting the same plasmid or virus will be integrated into their genomes (Jinek et al. 2012). This gives the Cas9 more target sequences at which to cleave and, theoretically, a more successful neutralization of the invasive DNA. The beauty of the Cas9 enzyme is that once the template DNA for Cas9 is in the target cell's genome, the enzyme can cut anywhere, and in multiple places, as long as a crRNA template(s) are provided.

Genome Editing versus Gene Silencing

In this study, gene silencing was the goal of the transfection process - mutation in the gene to either shift its reading frame into nonsense or produce a premature stop codon. However, another option exists - gene editing. This is done very similarly to gene silencing, where transfection occurs, introducing the Cas9 enzyme and two sgRNA constructs, resulting in two double-stranded breaks and excision of the area of interest. It also requires transfection of a repair template, as the major difference occurs in the repair process. Where single DNA breaks prefers the mutation-prone NHEJ (non-homologous end joining) process, DNA excision uses homologous recombination. Homologous recombination uses the transfected template to repair the break in a guided way. This template contains the gene edits. Single nucleotide differences can be introduced with a single break, and large portions of the gene can be rewritten with two breaks (caused by two differently targeted sgRNAs) (Ran et al. 2013).

With regards to CUL3, gene editing could be used to check the opposite of gene knockout - a knockin - by altering the promoter to turn the gene constitutively on. If a knockout results in slower growth, a knockin could result in accelerated growth. A knockin would likely

not demonstrate the same morphological changes seen in this study, as Aurora B function should be uninhibited, and potentially better. Knockin would also likely increase resistance of cells to CPT (camptothecin chemotherapy) by decreasing cellular TOP1 concentration.

Temporary CUL3 Knockout

The use of a catalytically inactive Cas9 has been seen to create a reversible knockout, or knockdown. The Cas9 still targets the gene of interest by way of sgRNA guidance, but instead of catalyzing a double-stranded break, the Cas9 will bind to the target site and inhibit transcription by simply getting in the way. Because no permanent mutation has occurred, the process, called CRISPRi, is reversible (Qi et al. 2013). This could allow the researcher to inhibit CUL3, and then remove the inhibition to see if the various phenotypes rectify themselves.

CUL3'S KNOWN ROLE IN CANCER

Database Results

CUL3 itself has been implicated as a driver gene in several types of human cancers, including head and neck squamous cell carcinoma; lung, stomach, and prostate adenocarcinoma; cutaneous melanoma; and esophageal carcinoma. In all cancers, the driver mutation resulted in a loss of function of CUL3 (IntOGen). Many of the mutations (72.5%, according to COSMIC) catalogued both by IntOGen and COSMIC result in a missense substitution mutation within the CUL3 gene. In addition to missense mutations of the gene itself, mutation in the neddylation protein Nedd8 has been found to affect cancer by way of controlling CUL3 function (IntOGen). The frequency of CUL3/Nedd8 mutation in any of the experiments reporting CUL3/Nedd8 mutation was no more than 3-4% of the genotyped cancers. While CUL3 does seem to have a role in driving cancer, it does so at a relatively infrequent rate.

IntOGen does not classify CUL3 as a driver gene for colorectal cancer. It does, however, reference the data found in COSMIC indicating that CUL3 is known to mutate in CRC. While the status of CUL3 as a driver gene in cancer is weak, CUL3 is still an intriguing therapeutic target and diagnostic tool.

Cancer Treatments

Substrates of CUL3 have been linked to the effectiveness of certain types of chemotherapies, giving CUL3 knockout cancers certain properties. CUL3 knockout makes it less likely that an individual will acquire resistance to antitumor camptothecins (CPTs), a type of chemotherapy. Sometimes, a cancer cell will become resistant to CPTs by down-regulating the expression of topoisomerase I (TOP1), the target of the drug. This is sometimes done by upregulating CUL3 and the ubiquitin-based degradation of TOP1 (Zhang et al. 2004B). Studies have shown that ubiquitination of TOP1 is an important determinant in CPT sensitivity (Beretta et al. 2013). This implies that inhibition of TOP1 degradation may be able to restore CPT sensitivity to resistant cancers. CUL3 knockout inhibits TOP1 degradation by removing the machinery to ubiquinate the TOP1, thus providing us with a potential avenue for rectifying CPT resistance.

Cyclin E cellular concentration has been inversely correlated with breast cancer patient survivability (Keyomarsi et al. 2002). Since cyclin E production is not really tissue specific, the likelihood is high that colon cancers would demonstrate the same trends seen in breast cancer. This indicates that a CUL3 knockout in colon cancer, which increases the cellular cyclin E by not degrading it, will likely result in more aggressive cancers and higher overall lethality.

Aurora B kinase overexpression has been recently correlated with lung cancer lethality (Takeshita et al. 2012). Again, Aurora B expression is also not tissue-specific, making the trends

seen in lung cancer likely to be seen in CRC. Aurora B overexpression is correlated with aneuploidy, or abnormal numbers of chromosomes, which often leads to increased malignancy (Masafumi et al. 2012). By inhibiting Aurora B chromosomal localization by CUL3 knockout, an Aurora B overexpression could be rectified.

Nrf2 expression has very recently been linked to gastric cancer and patient survivability. The higher the expression of Nrf2, the more aggressive the cancer (Kawasaki et al. 2015). In non-small-cell lung cancer, diallelic inactivation of KEAP1 (Nrf2's adapter protein), and therefore inhibition of Nrf2 degradation, results in higher rates of chemoresistance (Singh et al. 2006). A CUL3 knockout would increase expression of Nrf2, which should make the cancer more aggressive overall, and more resistant to oxidative stress. CUL3 overexpression has conversely been seen to decrease Nrf2 expression and increase breast cancer sensitivity to oxidative stress and chemotherapies (Loignon et al. 2009). In this way, CUL3 overexpression might become a therapeutic tool.

There is also the potential for utilizing the CUL3 ubiquitination mechanism as a type of target. For example, to ensure overexpression of a gene, like TOP1, one would only need to inhibit its adapter protein to turn off its degradation and increase cellular concentrations of TOP1 (Unfortunately, the adapter protein of TOP1 is as of yet undiscovered). CUL3's many substrates have different effects regarding cancer growth, many of which are contradictory to one another when it comes to cancer growth and patient survivability. Therefore, CUL3 is likely not a good target for cancer treatment, but rather its individual substrates are.

WORKS CITED

Andérica-Romero, A., González-Herrera, I., Santamaría, A., & Pedraza-Chaverri, J. (2013). Cullin 3 as a novel target in diverse pathologies. *Redox Biology, 1*(1), 366-372.

Beretta, G., Gatti, L., Perego, P., & Zaffaroni, N. (2013). Camptothecin Resistance in Cancer: Insights into the Molecular Mechanisms of a DNA-Damaging Drug. *Current Medicinal Chemistry, 20* (12), 1541-1565.

Buttke, T., Mccubrey, J., & Owen, T. (1993). Use of an aqueous soluble tetrazolium/formazan assay to measure viability and proliferation of lymphokine-dependent cell lines. *Journal of Immunological Methods, 157*, 233-240.

Canning, P., Cooper, C., Krojer, T., Murray, J., Pike, A., Chaikuad, A., . . . Bullock, A. (2013). Structural Basis for Cul3 Protein Assembly with the BTB-Kelch Family of E3 Ubiquitin Ligases. *Journal of Biological Chemistry, 288*(11), 7803-7814.

Colorectal Cancer. (2015). Retrieved March 15, 2014, from http://www.cancer.org/cancer/colonandrectumcancer/index

Copeland, N., & Jenkins, N. (2010). Harnessing transposons for cancer gene discovery. *Nature Reviews Cancer, 10* (10), 696-706.

Cortejoso, L., & López-Fernández, L. (2012). Pharmacogenetic markers of toxicity for chemotherapy in colorectal cancer patients. *Pharmacogenomics, 13*(10), 1173-1191.

COSMIC: Gene overview for CUL3. (2015). Retrieved March 13, 2015, from http://cancer.sanger.ac.uk/cosmic/gene/overview?ln=CUL3

CRISPR. (2015). Kyoto University Laboratory of Bacterial Infection. Retrieved April 7, 2015, from http://www.tmd.ac.jp/grad/bac/EnglishCRISPR.html

Denizot, F., & Lang, R. (1986). Rapid colorimetric assay for cell growth and survival. *Journal of Immunological Methods, 89,* 271-277.

Dupuy, A., Akagi, K., Largaespada, D., Copeland, N., & Jenkins, N. (2005). Mammalian mutagenesis using a highly mobile somatic Sleeping Beauty transposon system. *Nature,436*, 221-226.

Hanahan, D., & Weinberg, R. (2011). Hallmarks Of Cancer: The Next Generation. *Cell, 144*, 646-674.

Herceptin. (2015). Retrieved March 23, 2014, from http://www.herceptin.com/about

Hsu, P., Scott, D., Weinstein, J., Ran, F., Konermann, S., Agarwala, V., ... Zhang, F. (2013). DNA targeting specificity of RNA-guided Cas9 nucleases. *Nature Biotechnology, 31*(9), 827-832.

Hwang, H., & Clurman, B. (2005). Cyclin E in normal and neoplastic cell cycles. *Oncogene, 24*, 2776-2786.

Hwang, W., Fu, Y., Reyon, D., Maeder, M., Tsai, S., Sander, J., ... Joung, J. (2013). Efficient genome editing in zebrafish using a CRISPR-Cas system. *Nature Biotechnology, 31* (3), 227-229.

IntOGen - CUL3 gene cancer mutations. (2015). Retrieved April 8, 2015, from http://www.intogen.org/search?gene=CUL3

Ivics, Z., Hackett, P., Plasterk, R., & Izsvák, Z. (1997). Molecular Reconstruction of Sleeping Beauty, a Tc1-like Transposon from Fish, and Its Transposition in Human Cells. *Cell, 91*(4), 501-510.

Jinek, M., Chylinski, K., Fonfara, I., Hauer, M., Doudna, J., & Charpentier, E. (2012). A Programmable Dual-RNA-Guided DNA Endonuclease in Adaptive Bacterial Immunity. *Science, 337*(6096), 816-821.

Jinek, M., Jiang, F., Taylor, D., Sternberg, S., Kaya, E., Ma, E., ... Doudna, J. (2014). Structures of Cas9 Endonucleases Reveal RNA-Mediated Conformational Activation. *Science, 343*(6176), 1247997.

Kallio, M., Mccleland, M., Stukenberg, P., & Gorbsky, G. (2002). Inhibition of Aurora B Kinase Blocks Chromosome Segregation, Overrides the Spindle Checkpoint, and Perturbs Microtubule Dynamics in Mitosis. *Current Biology, 12*, 900-905.

Kawasaki, Y., Ishigami, S., Arigami, T., Uenosono, Y., Yanagita, S., Uchikado, Y., . . . Natsugoe, S. (2015). Clinicopathological significance of nuclear factor (erythroid-2)-related factor 2 (Nrf2) expression in gastric cancer. *BMC Cancer*.

Keyomarsi, K., Tucker, S., Buchholz, T., Callister, M., Ding, Y., Hortobagyi, G., ... Bacus, S. (2002). Cyclin E and Survival in Patients with Breast Cancer. *New England Journal of Medicine, 347*(20), 1566-1575.

Kobayashi, A., Kang, M., Okawa, H., Ohtsuji, M., Zenke, Y., Chiba, T., . . . Yamamoto, M. (2004). Oxidative Stress Sensor Keap1 Functions as an Adaptor for Cul3-Based E3 Ligase To Regulate Proteasomal Degradation of Nrf2. *Molecular and Cellular Biology, 24*(16), 7130-7139.

Loignon, M., Miao, W., Hu, L., Bier, A., Bismar, T., Scrivens, P., . . . Batist, G. (2009). Cul3 overexpression depletes Nrf2 in breast cancer and is associated with sensitivity to carcinogens, to oxidative stress, and to chemotherapy. *Molecular Cancer Therapeutics, 8*(8), 2432-2440.

Maerki, S., Olma, M., Staubli, T., Steigemann, P., Gerlich, D., Quadroni, M., ... Peter, M. (2009). The Cul3-KLHL21 E3 ubiquitin ligase targets Aurora B to midzone microtubules in anaphase and is required for cytokinesis. *The Journal of Cell Biology, 187*(6), 791-800.

Maerki, S., Beck, J., Sumara, I., & Peter, M. (2010). Finding the midzone: The role of ubiquitination for CPC localization during anaphase. *Cell Cycle, 9*(15), 2921-2922.

Mali, P., Yang, L., Esvelt, K., Aach, J., Guell, M., Dicarlo, J., ... Church, G. (2013). RNA-Guided Human Genome Engineering via Cas9. *Science, 339*, 823-826.

Murphy, S., Xu, J., & Kochanek, K. (2013). Deaths: Final Data for 2010. *National Vital Statistics Reports, 61*(4), 1-118.

Parry, G., & Estelle, M. (2004). Regulation of cullin-based ubiquitin ligases by the Nedd8/RUB ubiquitin-like proteins. *Seminars in Cell & Developmental Biology, 15*, 221-229.

Pintard, L., Willems, A., & Peter, M. (2004). Cullin-based ubiquitin ligases: Cul3–BTB complexes join the family. *The EMBO Journal, 23*(8), 1681-1687.

Qi, L., Larson, M., Gilbert, L., Doudna, J., Weissman, J., Arkin, A., & Lim, W. (2013). Repurposing CRISPR as an RNA-Guided Platform for Sequence-Specific Control of Gene Expression. *Cell, 152*(5), 1173-1183.

Ran, F., Hsu, P., Wright, J., Agarwala, V., Scott, D., & Zhang, F. (2013). Genome engineering using the CRISPR-Cas9 system. *Nature Protocols, 8*(11), 2281-2308.

Sander, J.D., Maeder, M.L., Reyon, D., Voytas, D.F., Joung, J.K., Dobbs, D. (2010) ZiFiT (Zinc Finger Targeter): an updated zinc finger engineering tool. Nucleic Acids Research, 38:W462-468

Singer, J., Gurian-West, M., Clurman, B., & Roberts, J. (1999). Cullin-3 targets cyclin E for ubiquitination and controls S phase in mammalian cells. *Genes & Development, 13*, 2375-2387.

Singh, A., Misra, V., Thimmulappa, R., Lee, H., Ames, S., Hoque, M., . . . Biswal, S. (2006). Dysfunctional KEAP1–NRF2 Interaction in Non-Small-Cell Lung Cancer. *PLoS Medicine, 3*(10), E420-E420.

Starr, T. K., Allaei R., Silverstein K.A.T., Staggs R.A., Sarver A.L., Bergemann T.L., … Largaespada D.A. (2009). A Transposon-Based Genetic Screen in Mice Identifies Genes Altered in Colorectal Cancer. *Science, 323*, 1747-1750.

Sukumari-Ramesh, S., Prasad, N., Alleyne, C., Vender, J., & Dhandapani, K. (2015). Overexpression of Nrf2 attenuates Carmustine-induced cytotoxicity in U87MG human glioma cells. *BMC Cancer, 15*(118), 1134-1144.

Sumara, I., Quadroni, M., Frei, C., Olma, M., Sumara, G., Ricci, R., & Peter, M. (2007). A Cul3-Based E3 Ligase Removes Aurora B from Mitotic Chromosomes, Regulating Mitotic Progression and Completion of Cytokinesis in Human Cells. *Developmental Cell, 12*, 887-900.

Takeshita, M., Koga, T., Takayama, K., Ijichi, K., Yano, T., Maehara, Y., . . . Sueishi, K. (2012). Aurora-B overexpression is correlated with aneuploidy and poor prognosis in non-small cell lung cancer. *Lung Cancer, 80*(1), 85-90.

Thompson, S., Loftus, L., Ashley, M., & Meller, R. (2008). Ubiquitin–proteasome system as a modulator of cell fate. *Current Opinion in Pharmacology, 8*(1), 90-95.

Van Gent, D., & Van der Burg, M. (2007). Non-homologous end-joining, a sticky affair. *Oncogene, 26*, 7731-7740.

Vogelstein, B., & Kinzler, K. (2004). Cancer genes and the pathways they control. *Nature Medicine, 10*(8), 789-799.

Voges, D., Zwickl, P., & Baumeister, W. (1999). THE 26S PROTEASOME: A Molecular Machine Designed For Controlled Proteolysis. *Annual Review of Biochemistry, 68*, 1015-1068.

Xu, L., Wei, Y., Reboul, J., Vaglio, P., Shin, T., Vidal, M., ... Harper, J. (2003). BTB proteins are substrate-specific adaptors in an SCF-like modular ubiquitin ligase containing CUL-3. *Nature, 425*, 316-321.

Zhang, D., Lo, S., Cross, J., Templeton, D., & Hannink, M. (2004A). Keap1 Is a Redox-Regulated Substrate Adaptor Protein for a Cul3-Dependent Ubiquitin Ligase Complex. *Molecular and Cellular Biology, 24*(24-), 10941-10953.

Zhang, H. F., Tomida, A., Koshimizu, R., Ogiso, Y., Lei, S., & Tsuruo, T. (2004B). Cullin 3 Promotes Proteasomal Degradation of the Topoisomerase I-DNA Covalent Complex. *Cancer Research, 64*(3), 1114-1121.

ACKNOWLEDGEMENTS

This work was funded by the Hamline University Summer Collaborative Undergraduate Research Program and the Hamline University Biology Department Lund Fund.

All data taken on the DLD-1 CRC cell line was done by Jen Scalze (Hamline University, Saint Paul MN) and Matthew Yang (Century College, White Bear Lake MN). All data taken on HT-29 was done by Maija Jedynak (North Hennepin Community College, Brooklyn Park MN) and Fathima Mohamed (Hamline University). This work was funded by the Howard Hughes Medical Institute.

APPENDIX

Appendix 1. Primer Sequences

Primer Name:	Sequence
CUL3Exon4P1.1F	aagttgcacattgcttaagatc
CUL3Exon4P1.1R	cctttccgctctcttgcaatc
CUL3Exon4P1.2F	atgctcacaagaactgtactc
CUL3Exon4P1.2R	ccaatgtgctcaacattcaaac
CUL3Exon11P2.1F	gagatcgtgccattgcattc
CUL3Exon11P2.1R	ggaaattgctgtatgccagg
CUL3Exon11P2.2F	caacgagcgaaactctgtc
CUL3Exon11P2.2R	gctccttttgatcacgagg
CUL3Exon14P3.1F	ggagcccattagtttgagac
CUL3Exon14P3.1R	catctggaaagtggaaacttg

Appendix 2. PCR Program

2 minutes	45 seconds	45 seconds	30 seconds	5 minutes
95°C	95°C	50°C	73°C	73°C

25 cycles

Appendix 3. Raw Observational Data

Cell Line	Guide Sequence	Growth Speed (approximate)	Abnormal Morphology?	Extra-Large Cells	Abnormal Adherence
Parental	None	Fast	No		
1FN1	C1	Fast	No		
1FN2	C1	Fast	No		
1FN3	C1	Fast	No		
1FN4	C1	Fast	No		
1MN1	C1	Medium	No		

1MY1	C1	Medium	Yes		X
1MY2	C1	Medium	Yes		X
1SY1	C1	Slow	Yes	X	
1SY2	C1	Slow	Yes	X	
1SY3	C1	Slow	Yes		X
1SY4	C1	Slow	Yes	X	
1SY5	C1	Slow	Yes	X	
1SY6	C1	Slow	Yes	X	X
1SSY1	C1	Super Slow	Yes	X	
1SSY2	C1	Super Slow	Yes	X	
1SSY3	C1	Super Slow	Yes	X	
2FN1	C2	Fast	No		
2FN2	C2	Fast	No		
2FN3	C2	Fast	No		
2FN4	C2	Fast	No		
2FN5	C2	Fast	No		
2MN1	C2	Medium	No		
2MY1	C2	Medium	Yes		X
2MY2	C2	Medium	Yes		X
2SY1	C2	Slow	Yes	X	X
2SY2	C2	Slow	Yes	X	
2SY3	C2	Slow	Yes		X
2SSY1	C2	Super Slow	Yes	X	
3FN1	C3	Fast	No		
3FN2	C3	Fast	No		
3FN3	C3	Fast	No		
3FN4	C3	Fast	No		
3FN5	C3	Fast	No		
3MN1	C3	Medium	No		
3MY1	C3	Medium	Yes		X
3MN2	C3	Medium	Yes	X	
3MY2	C3	Medium	Yes	X	X
3MY3	C3	Medium	Yes	X	X
3SY3	C3	Slow	Yes		X
3SY4	C3	Slow	Yes	X	
3SY1	C3	Slow	Yes	X	X
3SY2	C3	Slow	Yes	X	

Table 2. *Raw Data on Growth Speed and Abnormal Morphology*. Represented above is the categorization of individual cell lines from subcloning. Cell lines were assessed for relative growth speed, abnormal cell size, and abnormal flask adherence (either over-adhered or under-adhered).

Appendix 4. GoTaq Green Mastermix Protocols (Provided by Promega)

Promega

Usage Information

I. Standard Application

Reagents to be Supplied by the User

template DNA	downstream primer
upstream primer	mineral oil (optional)

1. Thaw the GoTaq® Green Master Mix at room temperature. Vortex the Master Mix, then spin it briefly in a microcentrifuge to collect the material at the bottom of the tube.
2. Prepare one of the following reaction mixes on ice:

For a 25µl reaction volume:

Component	Volume	Final Conc.
GoTaq® Green Master Mix, 2X	12.5µl	1X
upstream primer, 10µM	0.25–2.5µl	0.1–1.0µM
downstream primer, 10µM	0.25–2.5µl	0.1–1.0µM
DNA template	1–5µl	<250ng
Nuclease-Free Water to	25µl	N.A.

For a 50µl reaction volume:

Component	Volume	Final Conc.
GoTaq® Green Master Mix, 2X	25µl	1X
upstream primer, 10µM	0.5–5.0µl	0.1–1.0µM
downstream primer, 10µM	0.5–5.0µl	0.1–1.0µM
DNA template	1–5µl	<250ng
Nuclease-Free Water to	50µl	N.A.

For a 100µl reaction volume:

Component	Volume	Final Conc.
GoTaq® Green Master Mix, 2X	50µl	1X
upstream primer, 10µM	1.0–10.0µl	0.1–1.0µM
downstream primer, 10µM	1.0–10.0µl	0.1–1.0µM
DNA template	1–5µl	<250ng
Nuclease-Free Water to	100µl	N.A.

3. If using a thermal cycler without a heated lid, overlay the reaction mix with 1–2 drops (approximately 50µl) of mineral oil to prevent evaporation during thermal cycling. Centrifuge the reactions in a microcentrifuge for 5 seconds.
4. Place the reactions in a thermal cycler that has been preheated to 95°C. Perform PCR using your standard parameters.

II. General Guidelines for Amplification by PCR

A. Denaturation

- Generally, a 2-minute initial denaturation step at 95°C is sufficient.
- Subsequent denaturation steps will be between 30 seconds and 1 minute.

B. Annealing

- Optimize the annealing conditions by performing the reaction starting approximately 5°C below the calculated melting temperature of the primers and increasing the temperature in increments of 1°C to the annealing temperature.
- The annealing step is typically 30 seconds to 1 minute.

C. Extension

- The extension reaction is typically performed at the optimal temperature for *Taq* DNA polymerase, which is 72–74°C.
- Allow approximately 1 minute for every 1kb of DNA to be amplified.
- A final extension of 5 minutes at 72–74°C is recommended.

D. Refrigeration

- If the thermal cycler has a refrigeration or "soak" cycle, the cycling reaction can be programmed to end by holding the tubes at 4°C for several hours.
- This cycle can minimize any polymerase activity that might occur at higher temperatures, although this is not usually a problem.

E. Cycle Number

- Generally, 25–30 cycles result in optimal amplification of desired products.
- Occasionally, up to 40 cycles may be performed, especially for detection of low-copy targets.

III. General Considerations

A. GoTaq® Green Master Mix Compatibility

GoTaq® Green Master Mix is compatible with common PCR additives such as DMSO and betaine. These additives neither change the color of GoTaq® Green Master Mix nor affect dye migration.

If both agarose gel analysis and further downstream applications involving absorbance or fluorescence will be used, the two dyes can be removed from reactions using standard PCR clean-up systems such as the Wizard® SV Gel and PCR Clean-Up System (Cat.# A9281).

B. Primer Design

PCR primers generally range in length from 15–30 bases and are designed to flank the region of interest. Primers should contain 40–60% (G + C), and care should be taken to avoid sequences that might produce internal secondary structure. The 3´-ends of the primers should not be complementary to avoid the production of primer-dimers. Primer-dimers unnecessarily deplete primers from the reaction and result in an unwanted polymerase reaction that competes with the desired reaction. Avoid three G or C nucleotides in a row near the 3´-end of the primer, as this may result in nonspecific primer annealing, increasing the synthesis of undesirable reaction products. Ideally, both primers should have nearly identical melting temperatures (T_m); in this manner, the two primers should anneal roughly at the same temperature. The annealing temperature of the reaction is dependent upon the primer with the lowest T_m. For assistance with calculating the T_m of any primer, a T_m Calculator is provided on the BioMath page of the Promega web site at: **www.promega.com/biomath/**

C. Amplification Troubleshooting

To overcome low yield or no yield in amplifications (e.g., mouse tail genotyping applications), we recommend the following suggestions:

- Adjust annealing temperature. The reaction buffer composition affects the melting properties of DNA. See BioMath Calculator to calculate the melting temperature for primers in the GoTaq® reaction (www.promega.com/biomath/).
- Minimize the effect of amplification inhibitors. Some DNA isolation procedures, particularly genomic DNA isolation, can result in the copurification of amplification inhibitors. Reduce the volume of template DNA in reaction or dilute template DNA prior to adding to reaction. Diluting samples even 1:10,000 has been shown to be effective in improving results, depending on initial DNA concentration.
- Increase template DNA purity. Include an ethanol precipitation and wash step prior to amplification to remove inhibitors that copurify with the DNA.
- Add PCR additives. Adding PCR-enhancing agents (e.g., DMSO or betaine) may improve yields. General stabilizing agents such as BSA (Sigma Cat.# A7030; final concentration 0.16mg/ml) also may help to overcome amplification failure.

D. More Information on Amplification

More information on amplification is available online at the Promega web site: **www.promega.com/products/pcr/**

Part# 9PIM712
Printed in USA. Revised 3/12

Promega Corporation · 2800 Woods Hollow Road Madison, WI 53711-5399 U.S.A. · Toll Free in the USA 800-356-9526 · Telephone 608-274-4330 · Internet www.promega.com

Appendix 5. Lipofectamine Protocols (Provided by Invitrogen)

Lipofectamine® 2000 DNA Transfection Reagent Protocol

Transfect cells according to the following chart. Volumes are given on a per-well basis. **Each reaction mix is sufficient for triplicate (96-well), duplicate (24-well), and single well (6-well) transfections, and accounts for pipetting variations.** Adjust the amounts of components according to your tissue culture format. For additional information on scaling your transfection reaction, see page 1.

Timeline		Steps
Day 0	1 	**Seed cells to be 70–90% confluent at transfection**
	2 	**Dilute four amounts of Lipofectamine® Reagent in Opti-MEM® Medium**
Day 1	3 	**Dilute DNA in Opti-MEM® Medium**
	4 	**Add diluted DNA to diluted Lipofectamine® 2000 Reagent (1:1 ratio)**
	5 	**Incubate**
	6 	**Add DNA-lipid complex to cells**
Day 2–4	7 	**Visualize/analyze transfected cells**

Procedure Details

Component	96-well	24-well	6-well
Adherent cells	1–4 × 10^4	0.5–2 × 10^5	0.25–1 × 10^6
Opti-MEM® Medium	25 µL × 4	50 µL × 4	150 µL × 4
Lipofectamine® 2000 Reagent	1, 1.5, 2, 2.5 µL	2, 3, 4, 5 µL	6, 9, 12, 15 µL
Opti-MEM® Medium	125 µL	250 µL	700 µL
DNA (0.5–5 µg/µL)	2.5 µg	5 µg	14 µg
Diluted DNA Total	25 µL	50 µL	150 µL
Diluted Lipofectamine® 2000 Reagent	25 µL	50 µL	150 µL
Incubate for 5 minutes at room temperature.			
Component	**96-well**	**24-well**	**6-well**
DNA-lipid complex per well	10 µL	50 µL	250 µL
Final DNA used per well	100 ng	500 ng	2500 ng
Final Lipofectamine® 2000 Reagent used per well	0.2–0.5 µL	1.0–2.5 µL	5.0–12.5 µL
Incubate cells for 1–3 days at 37°C. Then analyze transfected cells.			

12 June 2013

For support, visit www.lifetechnologies.com/support.